THE COLLECTION OF AEROSOL PARTICLES BY CHARGED WATER DROPLETS

A THESIS

Presented to

The Faculty of the Division of Graduate

Studies and Research

By

Lonzy Lewis

In Partial Fulfillment

of the Requirements for the Degree

Master of Science in Physics

Georgia Institute of Technology

November, 1973

THE COLLECTION OF AEROSOL PARTICLES BY CHARGED WATER DROPLETS

Approved:

Michael J. Mattesoh, Chairman

L. David Wyly

Harry G. Dulaney

Date approved by Chairman: _____

ACKNOWLEDGMENTS

I would like to express my gratitude to my thesis advisor, Dr. Michael J. Matteson, for his direction and encouragement. I would also like to thank Mr. Edward Keng for his very helpful advice. Finally, I would like to thank my wife, Cynthia, for her patience, encouragement, and typing of the early drafts.

TABLE OF CONTENTS

	Page
ACKNOWLEDGMENTS	ii
LIST OF TABLES	iv
LIST OF ILLUSTRATIONS	v
SUMMARY	vi
Chapter	
I. INTRODUCTION	1
II. INSTRUMENTATION AND EQUIPMENT	8
III. PROCEDURE AND DATA ANALYSIS	17
IV. DISCUSSION OF RESULTS	23
V. CONCLUSIONS	46
VI. RECOMMENDATIONS	47
APPENDIX	48
1. Calibration of the Fluorometer	
2. Characterization of the Aerosol	
3. Derivation of the Capacitor Charging Curve	
4. Experimentally Measured Parameters	
5. Calculated Parameters	
BIBLIOGRAPHY	85

LIST OF TABLES

Table		Page
1.	Mass and Size Distribution of Aerosol	57
2.	Nomenclature	66
3.	Experimentally Measured Parameters	68
4.	Calculated Parameters	75

LIST OF ILLUSTRATIONS

Figure		Page
1.	Schematic Diagram of the Experimental Apparatus . . .	9
2.	Diagram of the Electrical Apparatus	11
3.	Diagram of the Aerosol Generator	12
4.	Diagram of the Deposition Chamber	14
5.	Graph of C_a vs. q^2 for F_a 600	30
6.	Graph of C_a vs. q^2 for F_a 970	32
7.	Graph of C_a vs. q^2 for F_a 1690	34
8.	Graph of C_a vs. q^2 for F_a 1350 and 1550	36
9.	Graph of E vs. K_I for F_a 600	38
10.	Graph of E vs. K_I for F_a 970	40
11.	Graph of E vs. K_I for F_a 1690	42
12.	Graph of E vs. K_I for F_a 1350 and 1550	44
13.	Optical Design of the Fluorometer	52
14.	Calibration Curve for the Fluorometer	53
15.	An Example of a Micro-Photograph	58
16.	Size Distribution of All Aerosol Particles	59
17.	Size Distribution of Large Aerosol Particles	60
18.	Size Distribution of Small Aerosol Particles	61
19.	Frequency Distribution of Aerosol Particles	62

SUMMARY

The collection of aerosol particles of geometric mean diameter 0.1 μm by charged water droplets was studied. The aerosol was generated from an aqueous solution containing 0.9% NaCl and 0.1% uranine by weight. The water droplets were charged by passing distilled water through a No. 24 hypodermic needle which was attached to a constant voltage source. They were formed in a chamber filled with aerosol which allowed collection of the particles on the droplet only during the formation period. As soon as the droplet was formed, it fell through a flushing air chamber into a collection chamber fitted with a grounded steel base. The collected water was withdrawn and analyzed for uranine by fluorometric techniques. By measuring the surface area and charge the amount of aerosol collected per droplet was correlated with the surface charge density. It was found that the amount of aerosol collected increased significantly with an increase in the surface charge density of the water droplets.

CHAPTER I

INTRODUCTION

During the last decade air pollution became recognized as a very serious problem in the United States. It was realized that each year greater and greater amounts of pollutants were being dumped into our environment. In an attempt to halt pollution, Presidential agencies were set up to establish and maintain limits on all types of emissions to the air. Much money has been spent and these agencies have been of significant aid; nevertheless, air pollution is still a growing problem today. Each year greater amounts of sulfur dioxide, the oxides of nitrogen, carbon monoxide, and particulate matter are pumped into the air. One important reason for this continued growth is that sufficient means of removing pollutants from stack gases have not been found. Studies have been made on the removal of sulfur and nitrogen from stack gases, but little work has been done on the removal of particulate matter from these gases.

With most of the anti-pollution systems in use today, some form of wet scrubbing is employed. In this process, a liquid, usually water, is brought into contact with the stack gas and the noxious gases are absorbed by the liquid. In almost every instant of wet scrubbing the purpose has been the removal of noxious gases from the stacks. Very little study has been made on the use of this method for the removal of particulate matter from the gas streams.

A great deal of effort has been spent investigating the collection of aerosol particles. Good reviews of the subject have been given by Fuchs (1), Davies (2), and Green and Lane (3). Early studies investigated the collection of aerosol particles on the inside walls of tubes and on plain surfaces. Wilson (4), Davies (5), and Fuchs and colleagues (6) have worked in this area. More work has been done in the area of deposition on cylindrical objects, due mainly to its immediate application to filtration. Zebel (7) and Natanson (8) have contributed significantly here. Very little study has been made on the deposition of aerosols on spheres, especially liquid spheres. However, Walton and Woolcock (9) investigated the collection of dust particles and Picknett (10) investigated the collection of salt particles by water sprays. Khimach and Shishkin (11) studied the collection of an aqueous mist on water drops being formed on glass beads. Pemberton (12) proposed a theory, which was latter tested under experiment by Oakes (13), for calculating the scavenging effects of rain on particulate matter suspended in the air. Additional study of the deposition of aerosol on spheres has been carried on by Fonda and Herne (14), and by Lundgren and Whitby (15). Fonda and Herne proposed a workable theory and Lundgren and Whitby arrived at an empirical equation for the deposition on spheres in a aerosol stream. Nevertheless, little of the mentioned work considered charged spheres and none considered charged liquid spheres. On the other hand, Gillespie (16) has made a review of the work done on the electric charge effects in aerosol phenomena. Still only one study in this review considered charged liquid spheres. This study was conducted by Gunn and Hitchfeld (17).

They observed the growth of 1.5 mm water droplets falling through an aerosol cloud. They observed no effect on the collection efficiency when each droplet carried an average charge of ± 0.2 esu. This charge was comparable to that found on rain droplets.

One study was found, however, which showed a definite effect of electric charge on the collection efficiency of aerosol particles on spheres. This study was done by Kraemer and Johnstone (18) and is reviewed here because of its importance to the present study. In this study of Kraemer and Johnstone, a theoretical solution and an experimental verification for the deposition of aerosol particles from a moving stream on spherical surfaces were given.

In the experimental part of this study, a LaMer-Sinclair generator was used to produce a dioctyl phthalate aerosol and three different size metal spheres were used. The aerosol was sent through a collecting cell for a timed period and permitted to deposit on the collecting sphere or to flow out the exhaust. At the end of this period the cell was swept clear of aerosol by a metered flow of air. The sphere was then removed and washed with ethyl alcohol. This alcohol solution was analyzed for dioctyl phthalate by ultraviolet absorption. Several different aerosols were used with diameters ranging from 0.54 - 1.18 μm, concentrations ranging from 3.3-193 mg/1, and aerosol velocities ranging from 1.56 - 6.89 cm/sec. The collection efficiency was calculated using the equation

$$E = (R_c/R)^2\left[1-\left(\frac{W - W_c}{W}\right)^{\frac{1}{2}}\right]$$

where R_c is the radius of the collection cell; R is the radius of the sphere; W is the mass flow rate of aerosol past the collector; and W_c is the rate of aerosol deposition on the collector. Measurements of E were made for both charged and uncharged collecting spheres. In the theoretical consideration, with the aid of a computer, the collection efficiency of aerosols for potential and viscous flows past a conducting sphere, due to the electrostatic forces, was calculated. Allowance was made for interception but inertial effects were neglected. Different dimensionless parameters, K_I, expressed the ratio of the electric force acting upon a particle located near the surface of the sphere to the quantity $6\pi NrU_o$, which characterizes the resistance of the medium to the motion of the particle, assuming the validity of Stokes' Law. Approximate relationships between the various parameters and the collection efficiency were determined.

The parameter, K_I, derived for induction to a charged sphere and uncharged aerosol was given by

$$K_I = \frac{X_s - 1}{X_s + 2} \frac{4 C r^2 q^2}{3 \epsilon_o R N U_0} \qquad (1)$$

where q surface charge density of the sphere

r radius of aerosol particle

R radius of sphere

X_s dielectric constant of sphere

ϵ_o permittivity of free space

C Cunningham factor

N viscosity of medium, and

U_0 relative velocity between collecting sphere and aerosol.

Similar parameters were given for the conditions: charged sphere and charged aerosol, K_E; and for charged aerosol and grounded sphere, K_G. The relationship between E and K_I was determined to be

$$E = \left(\frac{15\,\pi}{8} K_I\right)^{0.4} \qquad (2)$$

Experimental measurements of collection efficiencies obtained using the metal spheres were found to agree fairly well with the theory. As a result of this investigation a new type of dust collector was suggested: an electrified wet scrubber. For maximum collection in this scrubber the aerosol particles and the collecting surfaces were to be highly charged. The equation showed that collection by the electrostatic mechanism would be enhanced with increased times of retention in the dust collection equipment and with low relative velocities between the aerosol and collecting surfaces. As an example, the removal of 0.05 μm aerosol particles by charged water droplets was calculated. It was assumed that the aerosol carried an average charge of 4 electrons per particle and that the spray nozzles were charged to -5 KV. For 50 μm water droplets settling at 0.25 feet per second, the electrostatic parameter for induction to a charged sphere and charged aerosol, K_E, was found to be 830 and the collection efficiency of each spray droplet was 3320 times its projected cross sectional area.

Despite this interesting calculation and suggestion little work has been done to investigate directly the mechanism involved in the deposition of aerosol particles on charged water droplets. It is the

object of this study to shed some light in this area.

As mentioned previously, much work has been done on liquid-liquid and gas-liquid absorption. Although this work is not directly applicable here, some information can be gained from these studies. Early studies of mass transfer to droplets indicated three distinct stages or periods in the life time of drops and bubbles: the drop formation period, the free fall time, and the coalescence period (19). It was also discovered that mass transfer during the formation period contributed up to 50% of the total transfer (20). As a result of these findings mass transfer during drop formation has been the subject of many investigations. Lack of good experimental techniques for direct measurement of mass transfer during drop formation have limited the amount of information gained; but recently, Giardina (21) performed a study of the absorption of sulfur dioxide by charged water droplets during the formation period. In this study a special chamber was constructed which allowed deposition on the droplet only during the formation period. Since droplet formation is apparently a significant period in the overall deposition process, an apparatus very similar to that used by Giardina was selected to superimpose the present study of the surface charge density on the deposition of aerosols.

This research was then designed to investigate the effects of the surface charge density of water droplets on the deposition of a sodium chloride - uranine aerosol, to give the effects of different flow rates of the aerosol particles on the deposition, and to investigate the validity of the "Kraemer-Johnstone" theory derived for the deposition of an uncharged aerosol on a charged sphere. All of these

objectives were accomplished by applying a determined surface charge density to water droplets which were continuously being formed at the tip of a charged capillary that was exposed to an aerosol stream. As soon as the droplet fell from the capillary, contact with the aerosol ceased, and the droplets were collected for later analysis.

Although one significant industrial application of the phenomenon of deposition on charged water droplets has been stressed, this phenomenon may have useful applications elsewhere. Atmospheric scavenging of particulate matter may be one application. Some use may also be practical in inhalation therapy.

CHAPTER II

INSTRUMENTATION AND EQUIPMENT

The apparatus for the experiment was required to perform certain specific functions both reliably and accurately. The first function of the apparatus was to generate and charge droplets of water. Next, the water droplets had to be brought into contact with a dry aerosol in such a way that exposure would occur only during the drop formation period. Finally, the droplets had to be collected and analyzed. An additional requirement of the apparatus was the generation of the aerosol stream. A wet stream had to be generated, dried, and properly channeled such that measured amounts would be brought into contact with the water droplets. Measurements of the drop rate, the charging voltage and all flow rates were also required. A schematic diagram of the experimental apparatus is shown in Figure 1.

The experimental apparatus was composed of several sections according to function. One section consisted of the equipment needed to generate and charge the water droplets. It consisted of a polyethylene reservoir, a constant-head water pressure regulator, a stopcock, a hypodermic needle, and a high voltage supply. The pressure regulator was a plexiglass cup which maintained a constant pressure head of water by means of a drain outlet at a fixed height. The whole assembly could be moved vertically to achieve appropriate flow rates. Water flowed into the cup from the reservoir and left the cup by two

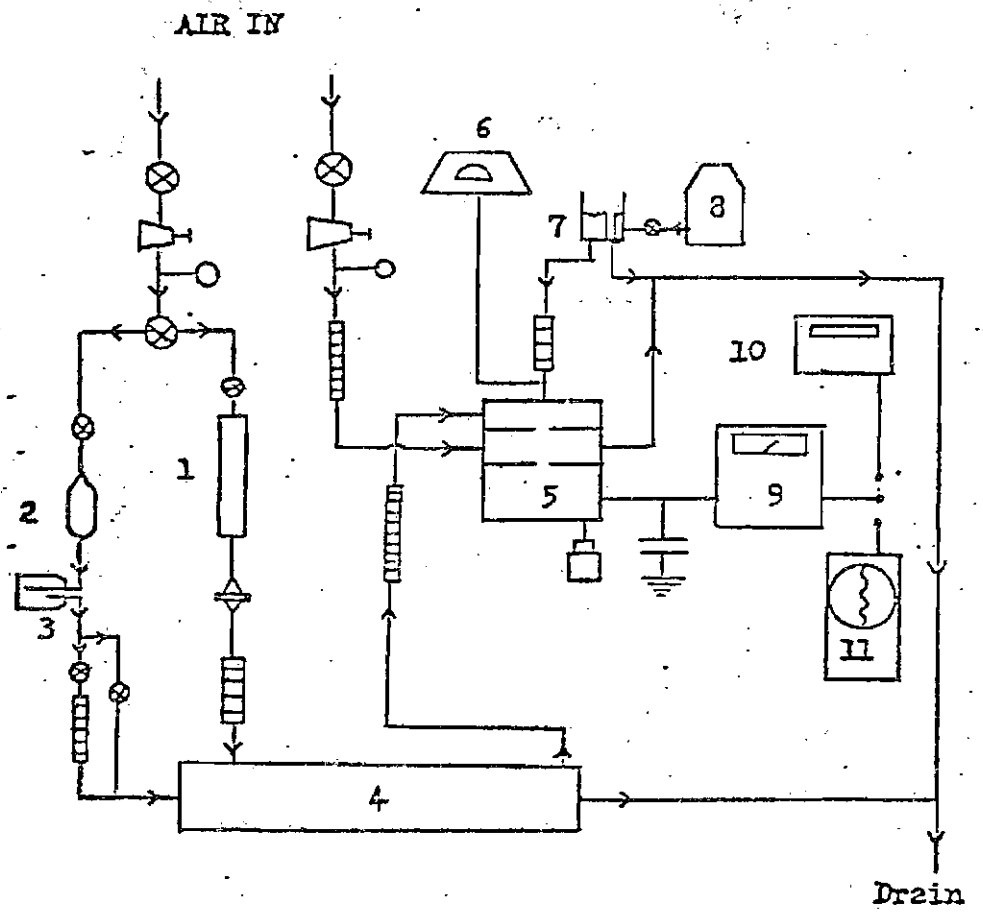

1 Silica Gel Column
2 Aerosol Generator
3 Collecting Flask
4 Dryer
5 Deposition Chamber
6 Voltage Source
7 Constant Head Pressure Regulator
8 H_2O Reservoir
9 Electrometer
10 Digital Voltmeter
11 Oscilloscope

Valve
Press. Reg.
Press. Indicator
Millipore Filter
Rotameter
Capacitor

Figure 1. Schematic Diagram of the Experimental Apparatus

means. Most of it left through the drain at the center of the cup and was later discarded. A much smaller amount left through an opening in the bottom of the cup and flowed through the needle to become droplets. The water used in the experiment was distilled water.

The droplets were formed by allowing water to flow through a No. 24 hypodermic needle which had been ground square and polished at the tip. The droplets were charged using a Beckman high voltage supply variable from 0-25kv which was electrically connected to the needle. The voltage supply was stabilized and protected against current drain by the high resistance, low pass filter diagrammed in Figure 2. The flow rate of water through the needle was monitored by a Matheson, Model 601 rotameter.

A second section of the experimental apparatus consisted of the equipment needed to generate and dry the aerosol. This equipment included a No. 40 DeVilbiss nebulizer or generator (Figure 3), several rotameters, and a dryer. Laboratory air was metered into the generator and continued through a collection flask and finally entered the dryer. A second supply of laboratory air flowed through a Millipore filter and a drying column of silica gel before entering the dryer. The dryer was a plexiglass cylinder, about 48 inches long and 2½ inches in diameter with several baffles along its length. The baffles provided good mixing of the two streams and removed most of the course particles from the mixture by impaction. Matheson No. 604 rotameters monitored both the wet aerosol stream and the dry air stream. Two streams left the dryer; one stream went directly to the drain while the other stream continued on to be contacted with the charged droplets in the deposition

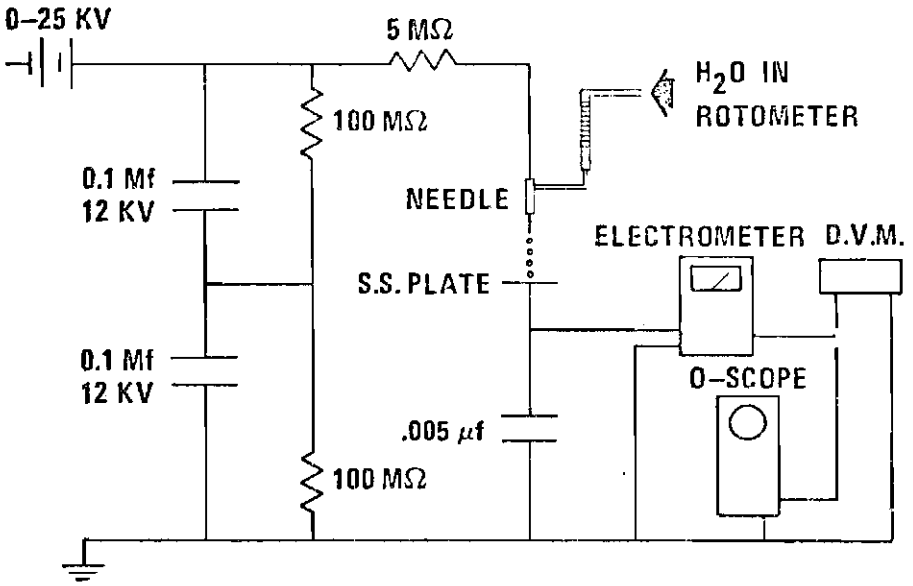

Figure 2. Diagram of the Electrical Apparatus

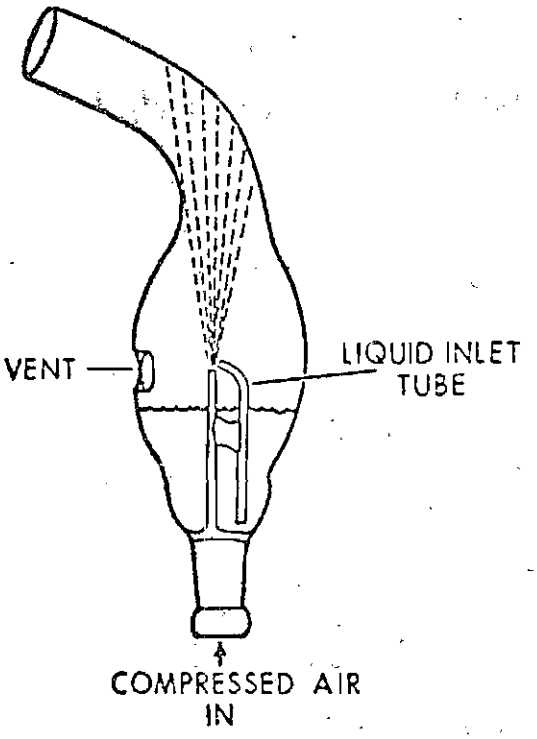

Figure 3. Diagram of the Aerosol Generator

chamber. This dry aerosol stream was monitored by a Matheson, Model 603 rotameter. Characterization of this dry aerosol is described in Appendix 2. A third supply of laboratory air was metered through a Millipore filter and entered the deposition chamber as flushing air. A Matheson, Model 604 rotameter monitored this stream. Both the dry aerosol stream and the flushing air stream left the deposition chamber by use of the flushing air exit and continued on to the drain.

The third section of the experimental apparatus is the deposition chamber itself (see Figure 4). It was a plexiglass cubical, 4 inches x 4 inches x 4 7/16 inches tall, composed of three compartments. The top compartment was the absorption chamber. This compartment was filled with the dry aerosol and was where the charged droplets contacted the aerosol. The middle compartment was the flushing chamber. Flushing air entered this compartment from its inlet side through a nozzle and left through a large outlet port located directly across the chamber from the inlet port. As the flushing air left the chamber it swept the dry aerosol stream along with it and continued on to the drain. The lower compartment was the collection chamber. The exposed charged droplets were collected in this compartment. The base of the collection chamber was a stainless steel plate fitted with a short stainless steel drain tube and was electrically connected to the outside. All metal-to-plexiglass joints were sealed with RTV sealant. The hypodermic needle was mounted in a Teflon plug which screwed into the top of the deposition chamber and served as electrical insulation. Droplets from the needle fell through concentric holes in the compartment dividers onto the stainless steel base plate

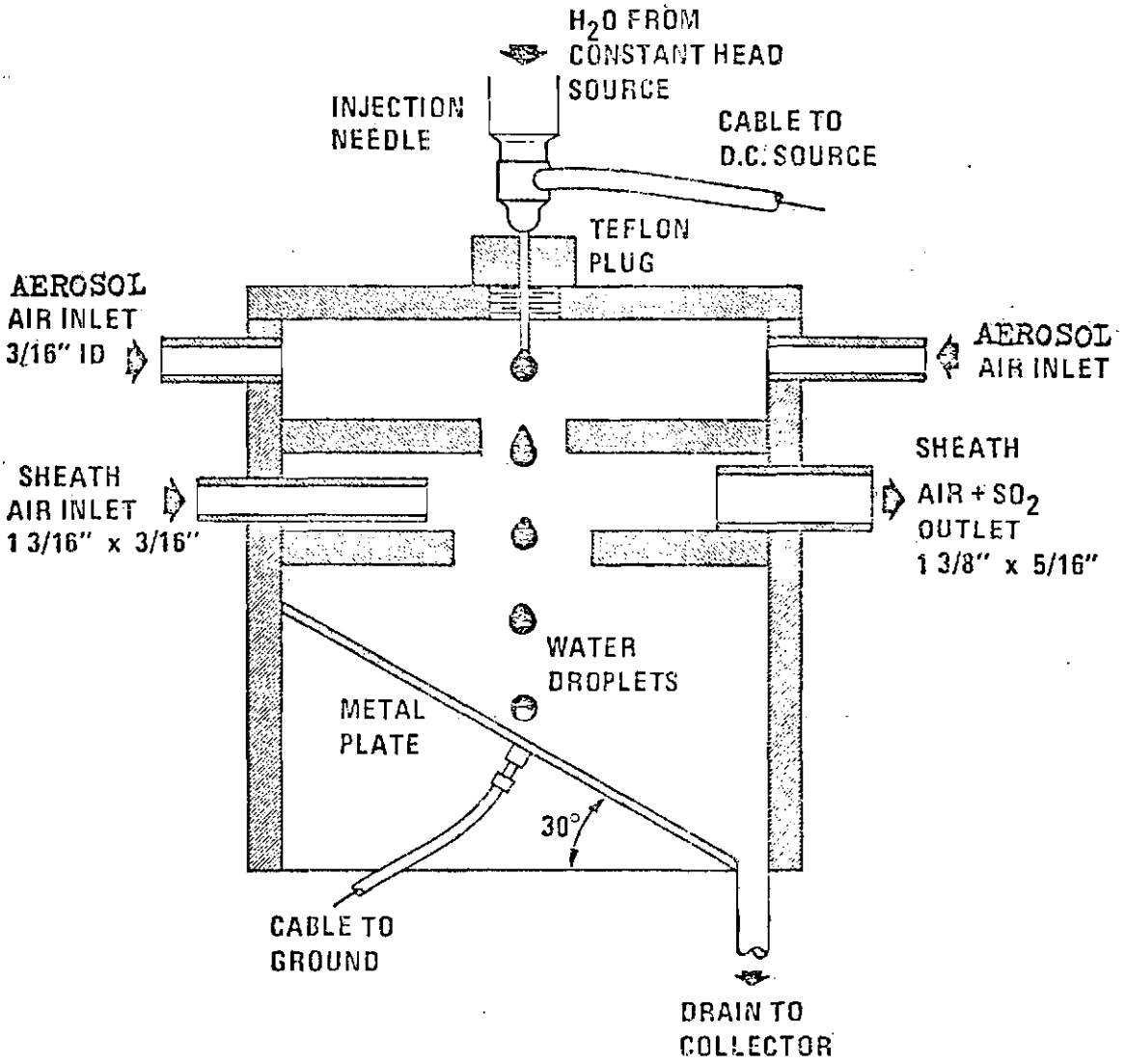

Figure 4. Diagram of the Deposition Chamber

of the collection chamber and then continued out the drain tube to a collection reservoir. The flushing air prevented any contact of aerosol with the water resting on the stainless steel plate.

A fourth section of the experimental apparatus consisted of the equipment and devices used to measure the droplet parameters. Included in this section were a Condensor Product glass capacitor, a Keithley, Model 6103A voltage divider, a Hewlett-Packard, Model 120 oscilloscope, a Honeywell digital voltmeter, a Standard timer, and a Matheson, Model 601 rotameter. The drop rate was measured using two methods. At low rates, the drops were counted visually and the time required for 50 drops to fall was measured with the timer. At high rates, when this method became inaccurate, the electrometer and oscilloscope were connected to the steel base plate. The electrometer served as a high gain amplifier such that when a charged droplet fell on the steel plate a visible signal was seen on the oscilloscope. The deposition chamber was covered with aluminum foil and grounded to block 60 cycle noise and to assure that the signals on the oscilloscope were sharp. To measure the charge delivered by the droplets, the steel plate was connected to the capacitor and the charge was stored by the capacitor. The voltage across the capacitor was monitored by the electrometer which was connected to the digital voltmeter. The RC time constant for the capacitive circuit was found to be 3410 ± 25 seconds. The voltage to the needle was measured by the electrometer in conjunction with the 1000:1 ratio voltage divider. The total applied voltage never exceeded 5 kv.

The fifth and last section of the experimental apparatus con-

sisted of the equipment used to collect and analyze the exposed charged droplets. This section was composed of several 50 ml beakers, several cuvets, and a Turner, Model 111, fluorometer and accessories. When sufficient water had collected in the collection reservoir below the collection chamber, a stopcock was opened and the collected water allowed to enter one of the beakers. Five milliliters of the collected water was then placed in a cuvet and analyzed by the fluorometer. The fluorometer is an instrument which measures the amount of fluorescence of a sample and is discussed further in Appendix 1. The amount of fluorescence is directly proportional to the amount of fluorescence material present in the sample. From this measurement the concentration of aerosol in the samples was determined.

The above description of the experimental apparatus does not explain fully the function of each piece of equipment but these functions will become clearer in the following chapters.

CHAPTER III

PROCEDURE AND DATA ANALYSIS

Prior to making an experimental test certain instruments required time for warm-up. The oscilloscope, electrometer, digital voltmeter, and fluorometer were all turned on and allowed a minimum of thirty minutes warm-up time. After this time, the aerosol stream and air streams were turned on and stabilized, and an appropriate water flow rate chosen. The high voltage source was also turned on and the voltage applied to the needle measured by means of the voltage divider and the electrometer. Next the fluorometer reading was set to zero for a pure distilled water sample (blank). Finally, all water which had collected in the collection chamber during this time was removed and discarded.

Immediately after draining the collection chamber the test was in progress. Flow rates of all streams were recorded and were constantly watched throughout the duration of a test. The drop rate was then measured. Next, the voltage gain across the capacitor was monitored by the electrometer with values being recorded every ten seconds for one minute. At this point flow rates were again checked for constancy and watched carefully until sufficient water had collected in the collection chamber. Once there was enough water, it was allowed to drain into a beaker. The reservoir was then again closed and preparation made for the next test.

The collected water was now ready for analysis. The fluorometer was checked for zero reading with the distilled water sample and adjustments made if necessary. Five milliliters of the collected water was placed in each of two cuvets, which were then placed, one at a time, in the fluorometer for analysis. A reading for each was taken and recorded. From these readings the concentration of aerosol in the collected water was determined by noting the concentration corresponding to the particular dial reading on the fluorometer calibration curve (Figure 14).

While the sample was being analyzed, the streams were achieving stability for the next test and when the analysis was complete, the next test could start upon drainage of the water from the collection chamber. The applied voltage and water flow rate were selected prior to the analysis of the sample. This completes the description of a typical experimental test.

After sufficient tests had been made the collected data was analyzed. Any errors present were either reading errors or systematic errors. The latter type arise from instruments out of calibration. In order to guard against this type of error, the instruments were checked against reliable standards. The electrometer was calibrated against the fixed voltage standard furnished by Honeywell for calibration of the digital voltmeter. The electrometer was found to be accurate. Comparison of the sweep time of the oscilloscope with a standard sixty cycle voltage source gave a correction factor of 1.011. The voltage divider was accurate. The air flow rotameters were calibrated by measuring a volume of gas which passed at a constant rate

by water displacement. The factory curves which accompanied the rotameters were accurate. The Model 601 rotameter, which measured the flow rate of water through the needle, was calibrated by observing the amount of water delivered in a given time. The glass capacitor was measured by means of a Wheatstone bridge circuit and found to have a capacitance of 4.88×10^{-9} farads at 1000 Hz. The RC time constant was determined to be 3410 ± 25 seconds, thus implying an electrical resistance of 6.98×10^{11} ohms, which was good isolation.

One important assumption was made in this experiment concerning the validity of the data obtained and will be discussed now. It was assumed that no aerosol was collected by the water resting on the steel plate of the collection chamber. In order to justify this assumption, samples that had been previously analyzed were rechecked, placed in the collection chamber again and allowed to remain there for the typical time of a test, viz., twenty minutes. Other than the water supply being shut off, the test was carried out in a normal manner. The water was then removed and analyzed once more. There was a measurable difference in the samples but the resultant points fell within the scatter already present in the data.

The manner in which the collected data was used to obtain the parameters of interest in this study will now be discussed. The notation used for both the measured and calculated parameters are listed in Table 2. The parameters of primary interest in the study were the surface charge density, q, and the amount of aerosol deposited per unit area of droplet, C_a. Of secondary importance were the collection parameter, K_I, and the collection efficiency, E.

In order to obtain the surface charge density, the radius of the droplet was needed. It was obtained from the expression

$$R = \left(\frac{3\ Vol}{4\ \pi}\right)^{1/3} \tag{3}$$

where the volume of the droplet, Vol, was obtained by dividing the volumetric flow rate of water, F_w, by the drop rate, DR.

The surface charge density q, was then calculated using

$$q = \frac{Q_0}{4\ \pi\ R^2\ (DR)} \tag{4}$$

where Q_0 is the charge delivery rate or current to the steel plate. The value of Q_0 was obtained from the capacitor charging curve

$$Q_0 = \frac{V_c}{R_s}\left[1 - \exp\left(-\frac{t_c}{R_s\ C_e}\right)\right]^{-1} \tag{5}$$

where R_s is the system resistance, V_c is the voltage across the capacitor at the time t_c, and C_e is the capacitance. The total charge on the droplet, Q, was obtained by dividing Q_0 by DR. Equation 5 is derived in Appendix 3.

The amount of aerosol collected per unit area of droplet, C_a, was obtained by observing the value of solute concentration corresponding to the fluorescence reading, FR, on the fluorometer calibration curve and dividing this value by both the number of droplets and the surface area of the droplets.

The number of drops, NOD, in each sample was obtained by dividing the volume of the sample by the volume of the droplet, Vol,

for that test. The sample volume was 5 ml in each case.

The relative velocity, U_0, between the droplet and the aerosol was taken as just the velocity at which the water was issued from the needle's tip. Since the aerosol entered the chamber on four sides through inlets located directly across the chamber from a second one, it was thought that the velocity of the aerosol particles was small compared with the velocity of the water entering the chamber. Indeed, the velocity of the aerosol stream was smaller than U_0 in every case. Thus U_0 was calculated by dividing the cross-sectional area of the needle's tip, A, by the flow rate of water through the needle, F_w.

The collection parameter, K_I, was obtained using Equation 1, repeated here

$$K_I = \left(\frac{X_s - 1}{X_s + 2}\right) \frac{4 C r^2 q^2}{3 \epsilon_o R N U_0}$$

The collection efficiency, E, was determined in the following way: the efficiency was defined as the ratio of the amount of aerosol collected when the droplet carried a surface charge, C_a, to the amount collected when there was no surface charge, C_0, that is, $E = C_a/C_0$. Thus E was equal to one when no surface charge was present. The value of C_0 varied little with the aerosol flow rate and had an average value of 0.3776 $\mu g/cm^2$.

The next topic of discussion is the error produced in the calculated results by random error associated with the reading of instruments scales. The surface charge density, q, was a function of V_c, R_s, t_c, DR, F_w, and C_e. To a fair approximation, the standard

deviation in q is equal to the square root of the sum of the squares of the standard deviations of the parameters involved (22). The deviations are

$$d(C_e) = 0.2\% \qquad d(V_c) = 1\%$$

$$d(R_s) = 0.8\% \qquad d(t_c) = 1\%$$

$$d(DR) = 0.3\% \qquad d(F_w) = 1.5\%$$

$$\therefore d(q) = 2.5\%$$

The amount of aerosol collected, C_a, was a function of FR, F_w, and DR. Since the variation in F_w and DR will cancel for the most part, the contribution of each of these will be reduced by one-half. The calibration curve was a least square fit, so the error involved in this calculation should also be included. These deviations are

$$1/2\ d(F_w) = 0.75\% \qquad d(FR) = 0.5\%$$

$$1/2\ d(DR) = 0.15\% \qquad d(Lsq) = 0.1\%$$

$$\therefore d(C_a) = 0.9\%$$

The collection parameter, K_I, was a function of q, r, F_w, and DR. The approximate deviations here are

$$d(q) = 2.5\% \qquad d(r) = 2.33\%$$

$$d(F_w) = 1.5\% \qquad d(DR) = 0.3\%$$

$$\therefore d(K_I) = 6.29\%$$

CHAPTER IV

DISCUSSION OF RESULTS

The experimentally measured parameters for all tests are listed in the Appendix 4. The calculated parameters for all tests are listed in Appendix 5. The first twenty tests were considered void, for fluctuations in the system were extremely high during the tests. Improvements were made on the system and the remaining tests are listed in the appendices mentioned. A few of these tests also produced bad points. They, however, were no eliminated from the list of values. Graphic representations of the results are incorporated within this chapter.

Before describing the individual graphs, however, some general remarks about the data are in order. First, an aerosol cloud, being composed of course particles of various sizes compared with a gas, makes experimentation difficult, especially in an experimental configuration like the one employed in this study. Large distances between the aerosol generator and the reaction chamber allow much time for coagulation of the particles, lost of particles to the walls of tubing, clogging of the lines and thus changes in the flow rates. Fluctuations in the air flow rates were not noticeable in this study but there were fluctuations in the aerosol flow rate. Some were as large as six percent of the mean value at high flow rates. Such fluctuations were kept at a minimum, however, and at low rates the

fluctuations were very small. The water flowrate also changed slightly from test to test. This variation, however, was on the order of one percent of the mean value and no special accounting for this changed was made. Secondly, it is well known that any foreign material as well as the desired component is liable to give a fluorescence reading. Although distilled water was used exclusively in the experiments, it was not known if any corrosion products had entered the water stream from the stainless steel hypodermic needle and stopcock. It should be recalled that this combination was being subjected to high voltage of both polarities throughout the trials. Such an error was assumed small, since both the stopcock and needle were cleaned prior to every series of tests. Nevertheless, since most aerosols are naturally charged, the exposed needle was a site of heavy deposition of particles when high voltage was applied to the needle. It was not known if, when a lesser voltage was applied following a test in which a higher voltage had been applied, some of the particles which had been deposited on the needle were knocked off through collisions with other aerosol particles in the stream and then deposited on the droplets being formed or on those in the collection chamber. The electrostatic attraction was, of course, no longer as strong as in the preceding test. This occurrence, also, was thought to be of little importance since the flushing air stream was assumed to be effective in sweeping out the unused aerosol particles. This assumption, however, was not strictly true for some aerosol was deposited on the water in the collection chamber. This fact was verified by placing plain distilled water in the collection chamber and letting it remain there for the time of a

typical test, and analyzing it afterwards. The amount deposited in the collection chamber was comparable to the amount obtained for zero charge on the droplets and probably distorts the results at small surface charge densities.

Another point of interest is that the distilled water in the reservoir above the needle was found to become positively charged after a test in which high voltage had been applied to the needle. This was true for applied voltages of either polarity. The amount of charge on the water changed very little with the applied voltage of the preceding test. However, prior to making any tests with high voltage, the water was found to carry very little charge or no charge at all. This occurrence was not studied in depth and no explanation of it is attempted here. In the early tests the deposition with zero charge on the droplets was taken first and later rechecked. However, when the check was made the voltage gain was not monitored and it was not known if the droplets were charged. In the latter part of the study the voltage gain for all tests was monitored.

Still another point of considerable interest is the fact that the amount of solution in the aerosol generator changed with time. As time passed the solution became evaporated and more concentrated and thus the mass distribution of the aerosol probably changed with time. This change was controlled to a certain extent by placing new solution in the generator after it reached a certain volume. No correction in the data was made for this occurrence.

Finally, it should be mentioned that any kind of foreign material either in the water to be analyzed or on the cuvets, even fingerprints,

could alter the results obtained significantly. This effect was not calculated in any way although every practical precaution against the accidental insertion of foreign materials in the sample or on the cuvets was taken. All of the above points were mentioned for these occurrences, along with other unseen ones, may account for some of the scatter in the data. With these remarks in mind the explanation of the various curves can proceed.

The data representing the effect of surface charge on the deposition of aerosol is presented in Figures 5, 6, 7, and 8. Each figure is entitled C_a vs. q^2. These figures show the relationship of C_a to q^2 for different aerosol flow rates. As these graphs show, there is a significant increase in the amount of deposited aerosol with increasing surface charge on the droplets. The exact relationship, however, was not determined. There is a slight increase in the amount of aerosol deposited when positive voltage was applied compared to when negative voltage was applied. Figure 7 shows a more noticeable increase than the other figures. This increase in deposited aerosol for positive voltages may be explained in light of a study done by Chow and Mercer (23). It is a known fact that droplets formed by atomization are usually charged. Chow and Mercer studied the charges on the aerosol particles generated from sodium chloride-uranine solutions. For a 1% solution, 0.9% NaCl and 0.1% uranine, it was found that more negative charge carriers were produced than positive ones. The ratio of negative mass to positive mass was found to be 1.07. This ratio, however, changed for solutions of different concentrations. Since the aerosol used in the present study was also generated from a 1% sodium

chloride-uranine solution, it is believed that the increase in collected mass for positive charged droplets over that of negative ones may be accredited to the greater amount of negative particles in the aerosol.

There are variations in the results for data taken at different times, evident in Figures 6 and 7. Data for different times were denoted by a separate symbol when it differed significantly from the rest of the data. The relative velocity, U_0, during each set of data points is indicated on the graphs. It may be noted that where differences exist in data taken at different times, there exist also a difference in U_0. Besides these differences, however, there is still a significant amount of scatter in the data. Some reasons for this scatter may be found in studies done previously. Walton and Woolcock (9), for example, noted that the collection of dust particles of diameter less than 2.5 μm was very hard to measure experimentally. In this study no charge effect was present. However, Gunn and Hitschfeld's study (17) showed that collection of particles of diameter about 15 μm had only 15% efficiency and implied that the efficiency decreased with the particle diameter. In this study charged droplets were used. Hence, the size of the aerosol particles in the present study (0.1 μm) may be a significant factor in the results obtained.

The next topic of interest is the relationship between the collection parameter K_I and the collection efficiency E. Both E and K_I are listed in Table 4. Figures 9, 10, 11, and 12 show graphical representations of these values. Also shown in these figures is the theoretical efficiency predicted by Kraemer and Johnstone (18). As can be seen from the figures the measured efficiences were larger than the

the theoretical ones in every case. The experimental data was least square fitted to straight lines. The slopes of these lines were greater than those of the theoretical curves for all data. However, the collection efficiency found in this study was obtained in a manner totally different from the one used by Kraemer and Johnstone. This fact, no doubt, accounts for the large values of the experimental E's. The experimental setup used in the present study did not permit the calculation of E in the manner used in Kraemer and Johnstone's study. The values of the theoretical efficiency was on the order of 10^{-1} in magnitude while the experimental efficiency was on the order of 10. Thus, to make a comparison of the theory and experiment, the slopes of the theoretical curves were multiplied by 10^2 so that both efficiencies were of the same magnitude. After this procedure, the slopes of the theoretical curves were larger than the experimental ones in every case. The absolute difference in the slopes of the theoretical and experimental curves were then calculated. The absolute difference in slopes for negative charge on the droplets ranged from 0.84 - 2.14 and had an average value of 1.53. These differences for positive values of charge ranged from 0.20 - 1.20 and had an average value of 0.75. There are several possible reasons besides the scatter in the data for the differences in the theoretical and experimental values. First, the aerosol used in this study carried a natural charge and such particles near a charged collector are influenced by both K_I and $-K_E$. Thus the real collection parameter should be represented by $K = K_I - K_E$, for some of the particles were being repelled while others were being attracted. Secondly, Kraemer and Johnstone also noted greater deviation

from the theory for the data obtained investigating K_I, despite using the corrected parameter K. Moreover, they noted that for low collection efficiencies and small values of the parameters, the theory over estimates the collection efficiency. Although these differences exist, the slopes of the experimental lines do not differ greatly from those of the theoretical curves considering the scatter and low values of K_I.

In conclusion, the results obtained in this study demonstrate pronouncedly the effect of surface charging of water droplets on the deposition of aerosol particles. The results also show that the theory of Kraemer and Johnstone may be used to approximate the collection efficiences of aerosol particles on charged liquid spheres.

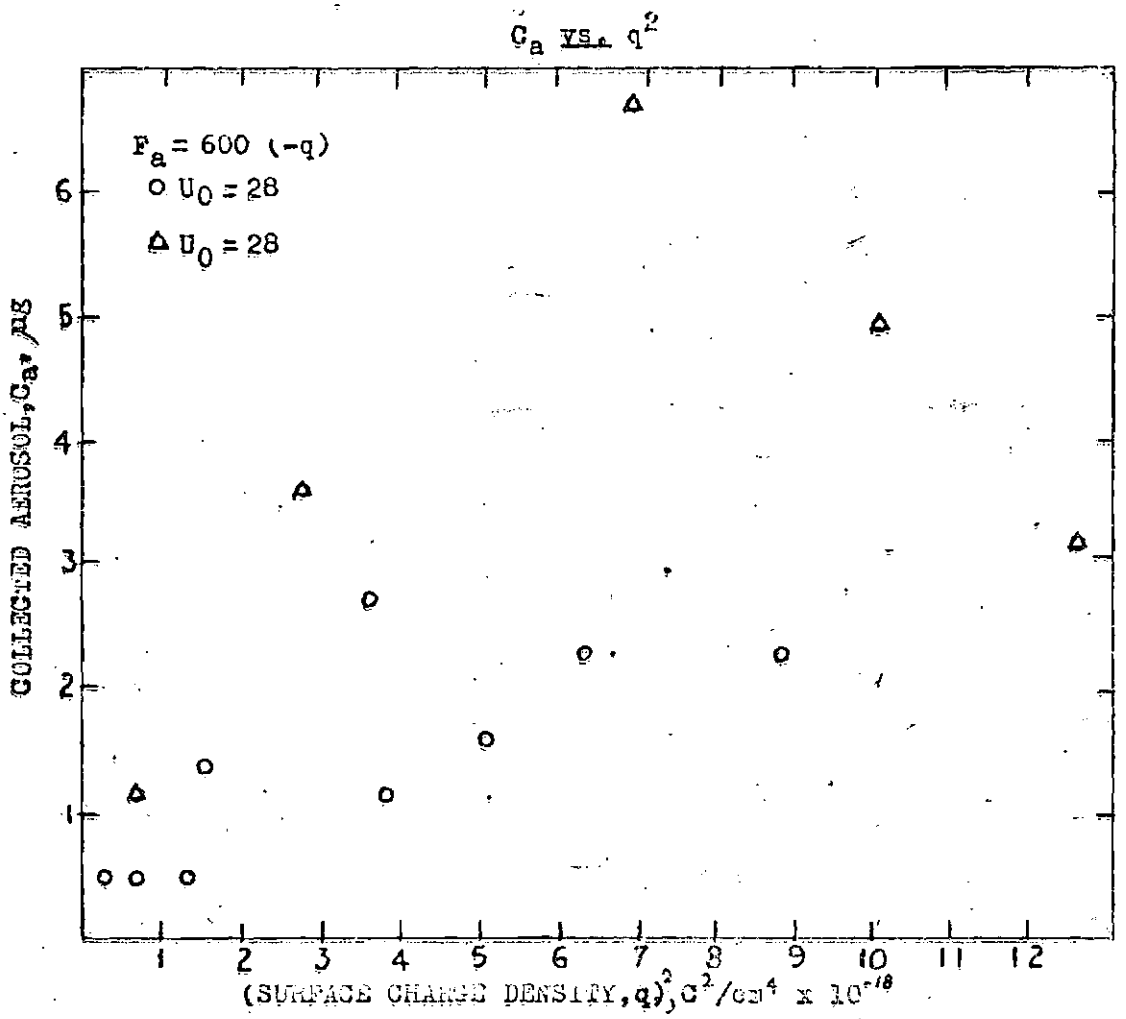

Figure 5a. Graph of Collected Aerosol vs. Surface Charge

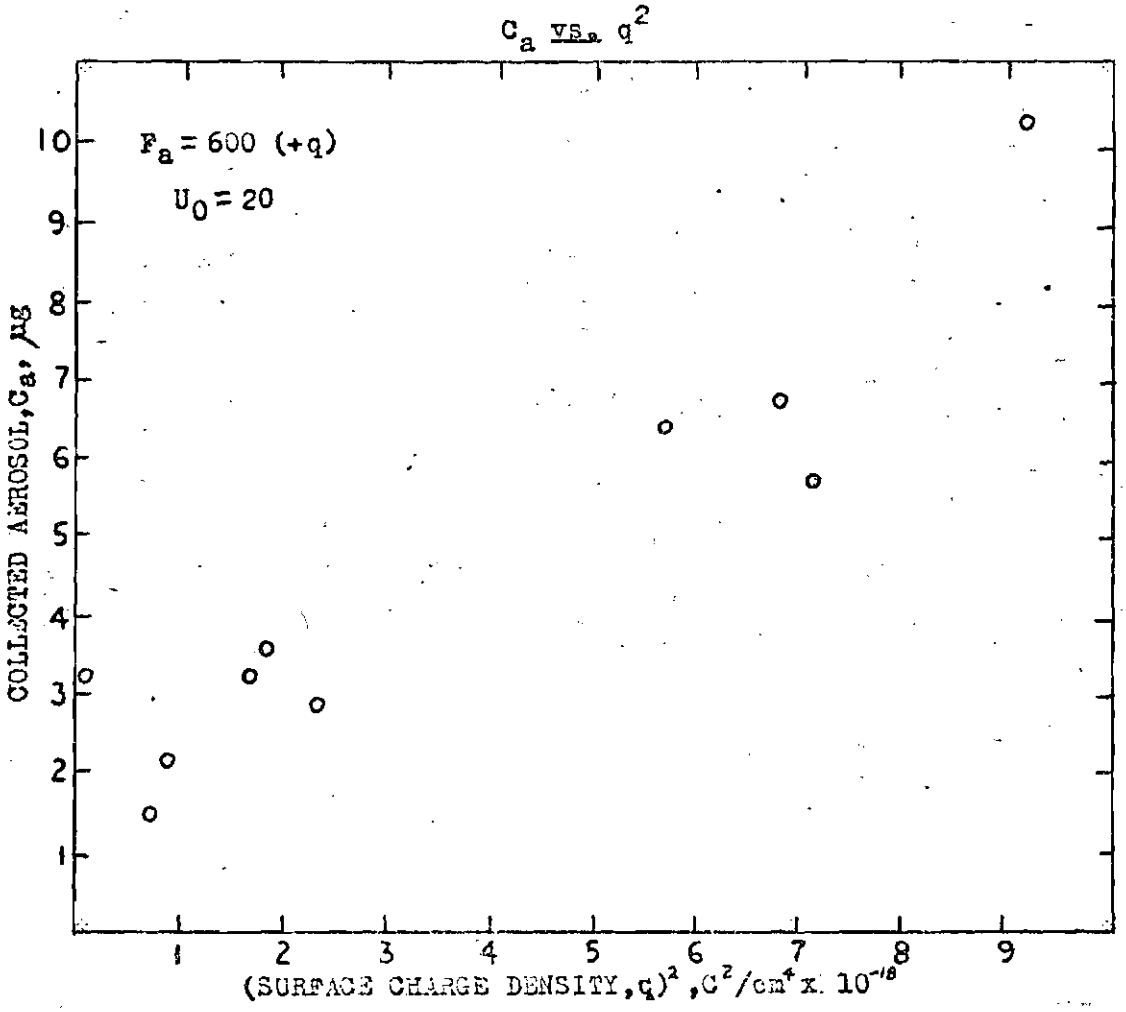

Figure 5b. Graph of Collected Aerosol vs. Surface Charge

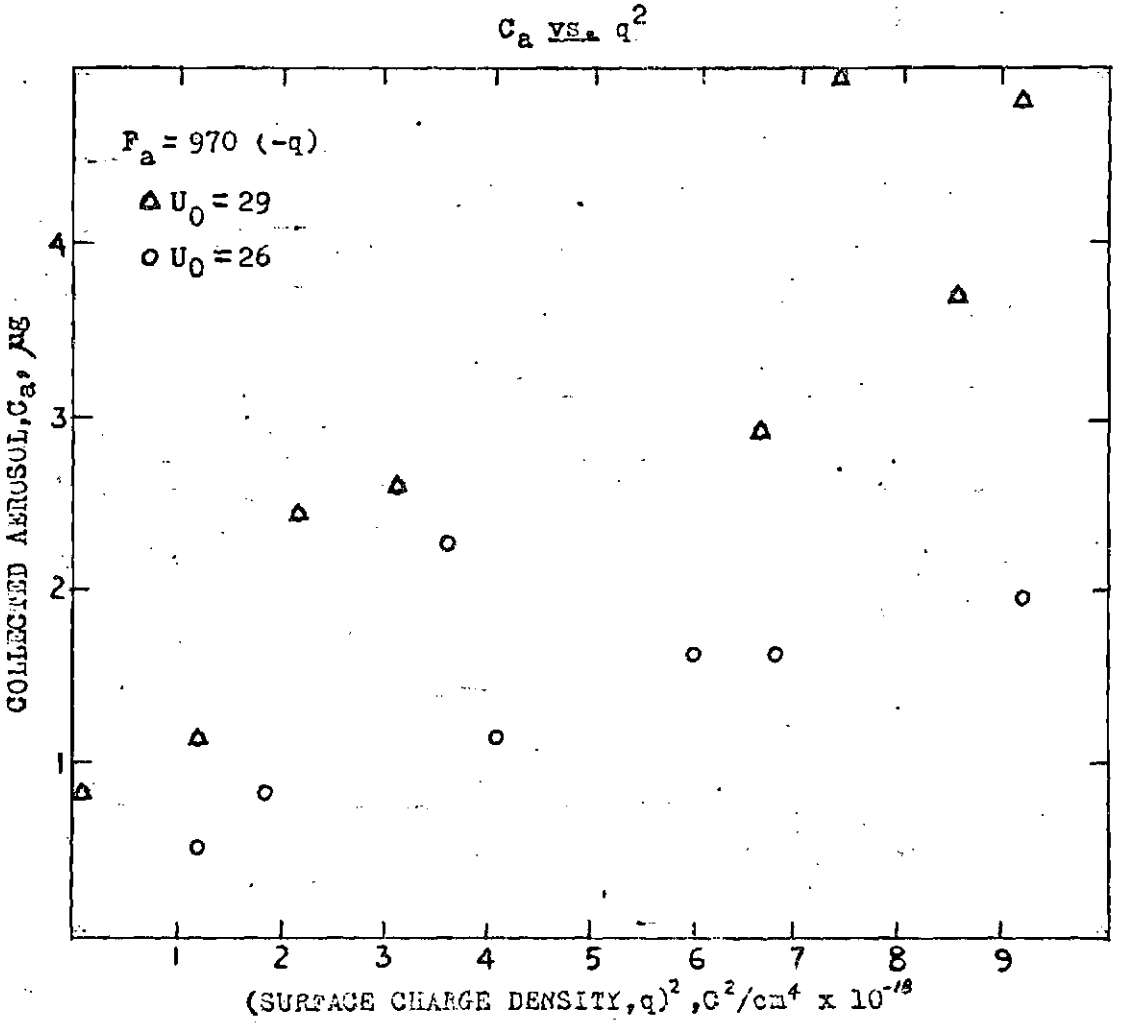

Figure 6a. Graph of Collected Aerosol vs. Surface Charge

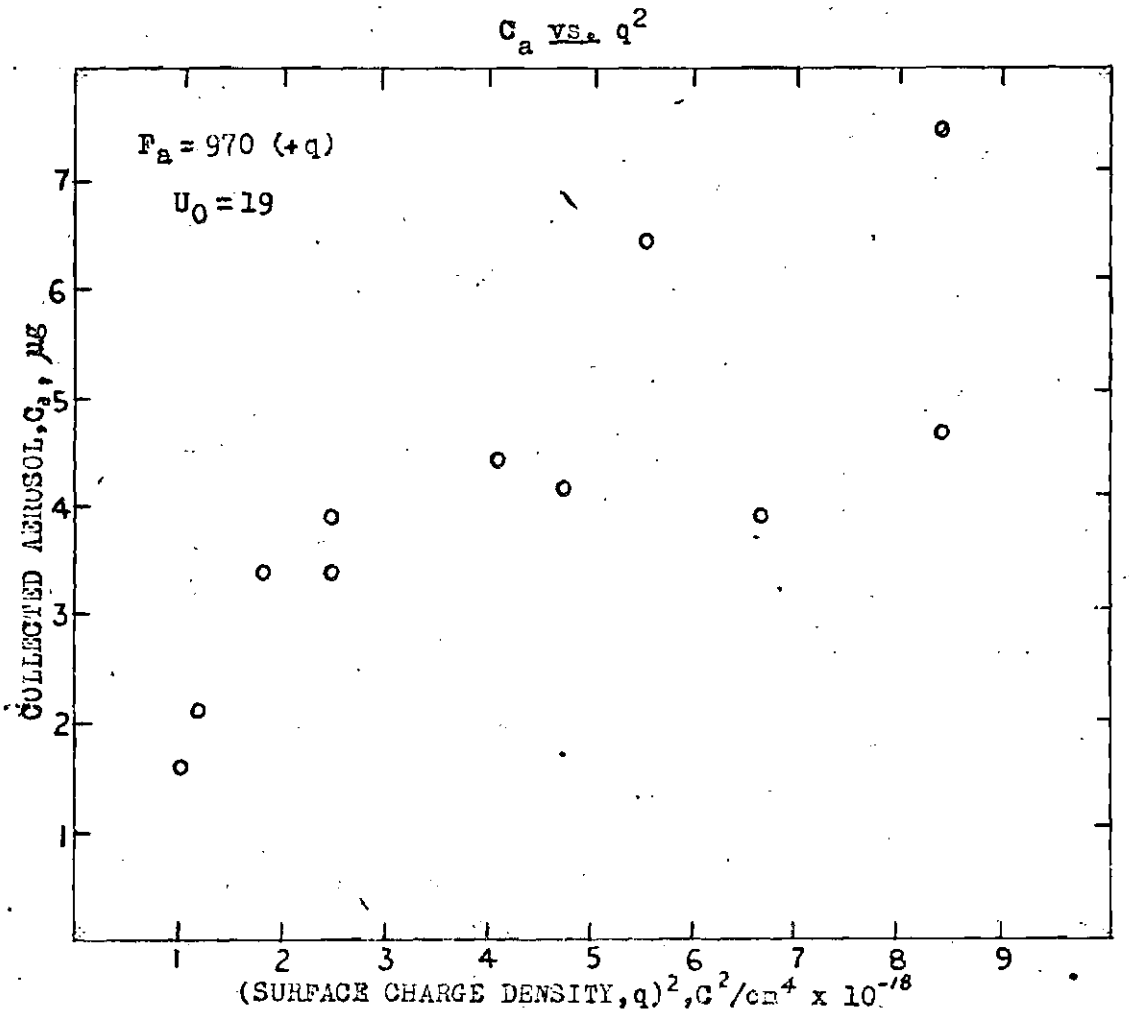

Figure 6b. Graph of Collected Aerosol vs. Surface Charge

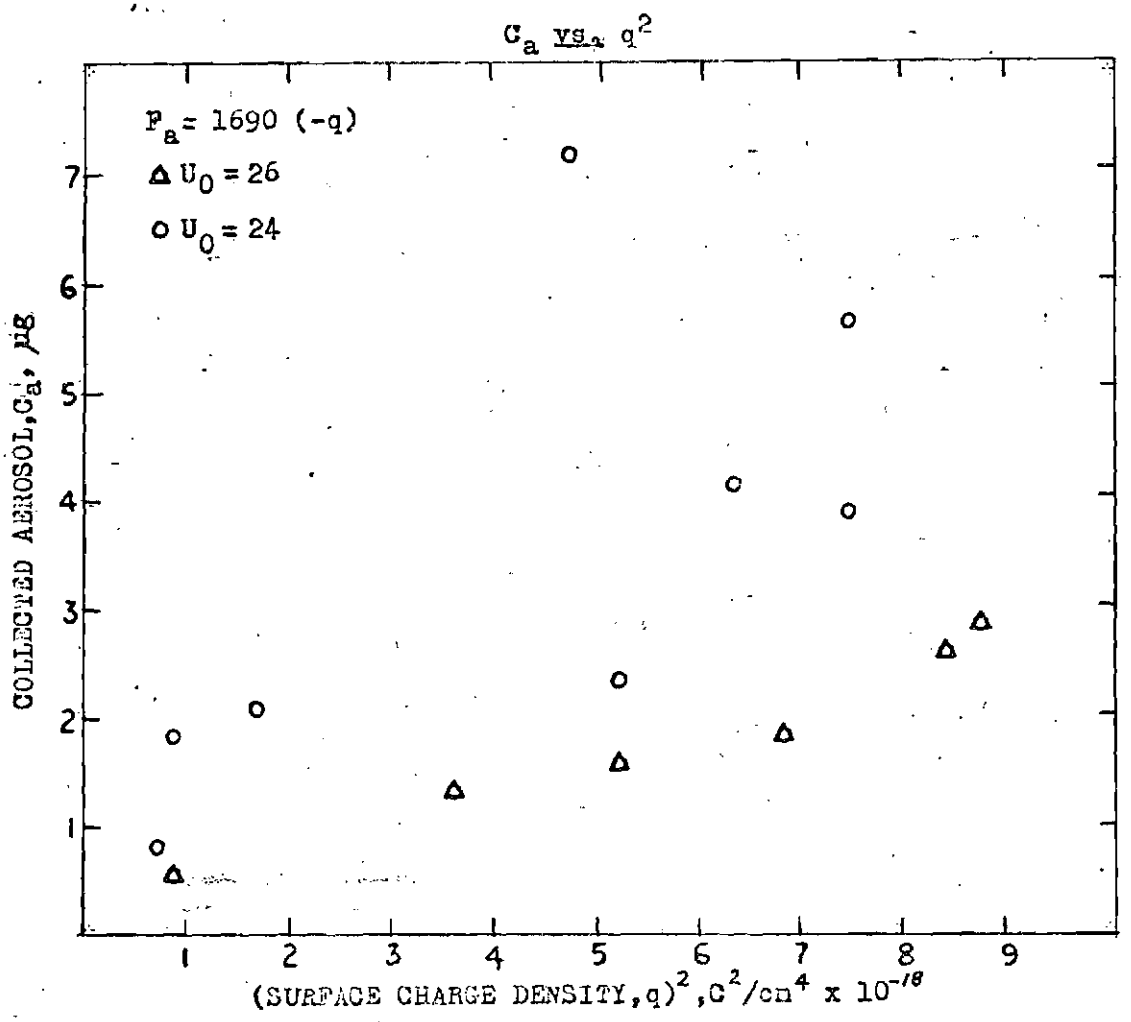

Figure 7a. Graph of Collected Aerosol vs. Surface Charge

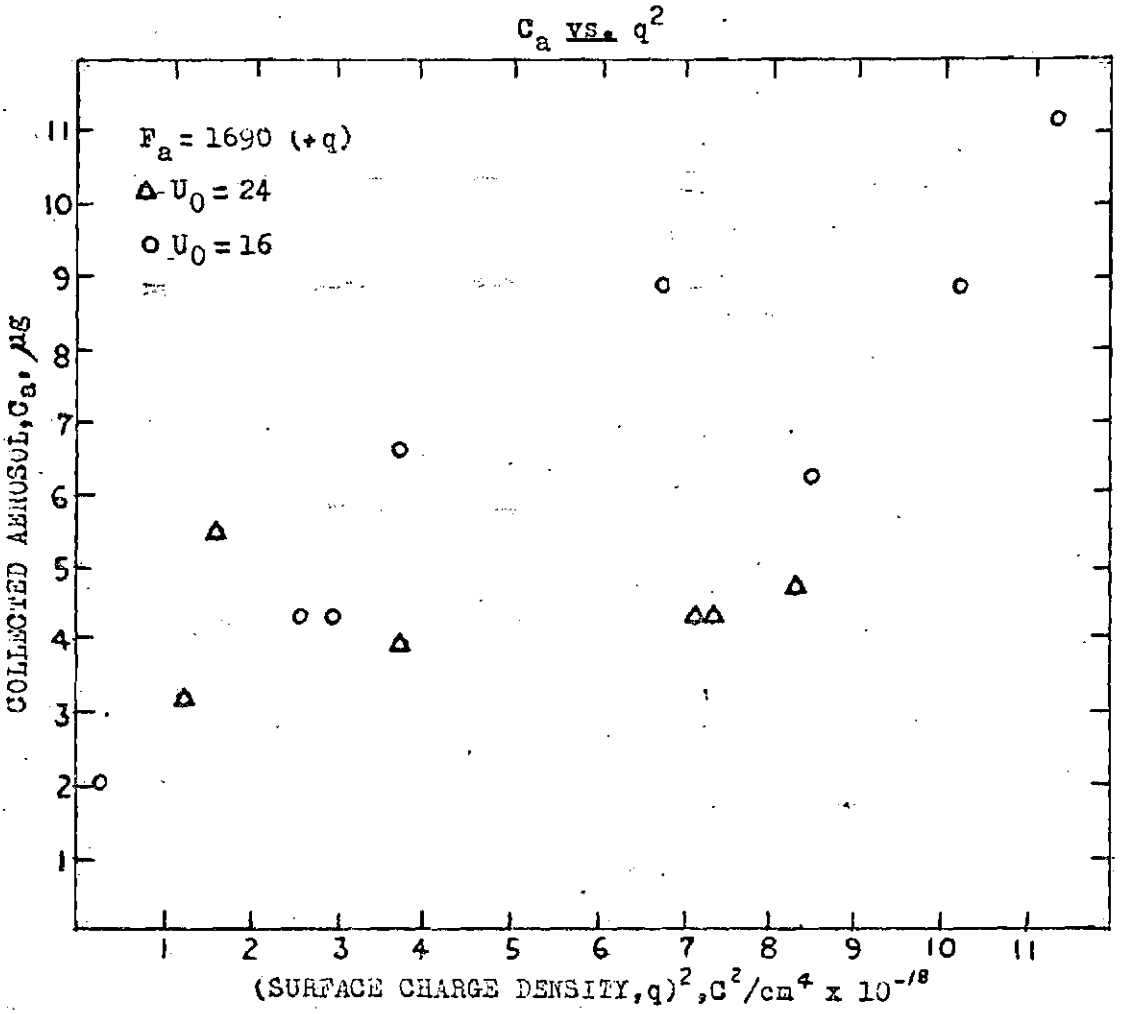

Figure 7b. Graph of Collected Aerosol vs. Surface Charge

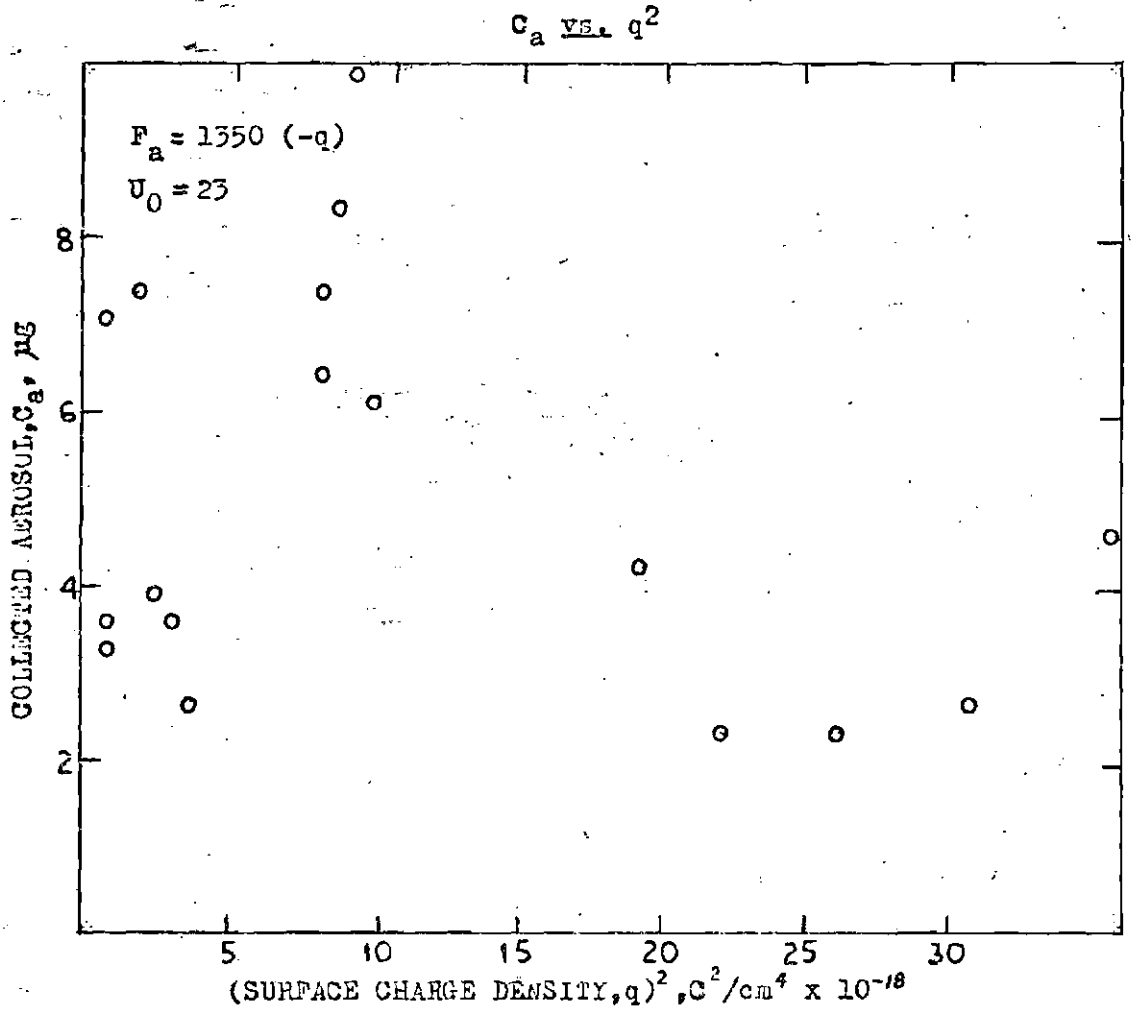

Figure 8a. Graph of Collected Aerosol vs. Surface Charge

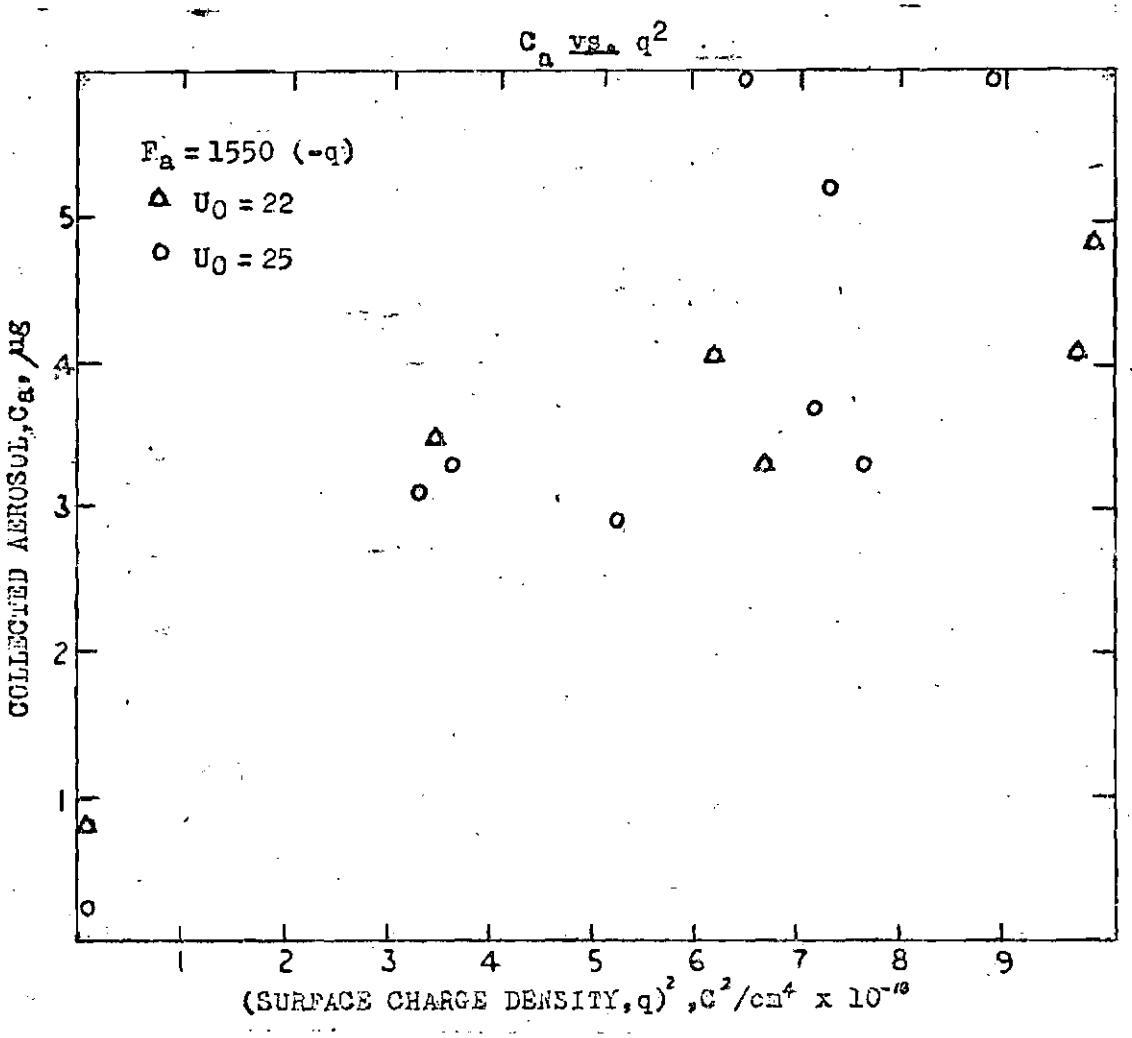

Figure 8b. Graph of Collected Aerosol vs. Surface Charge

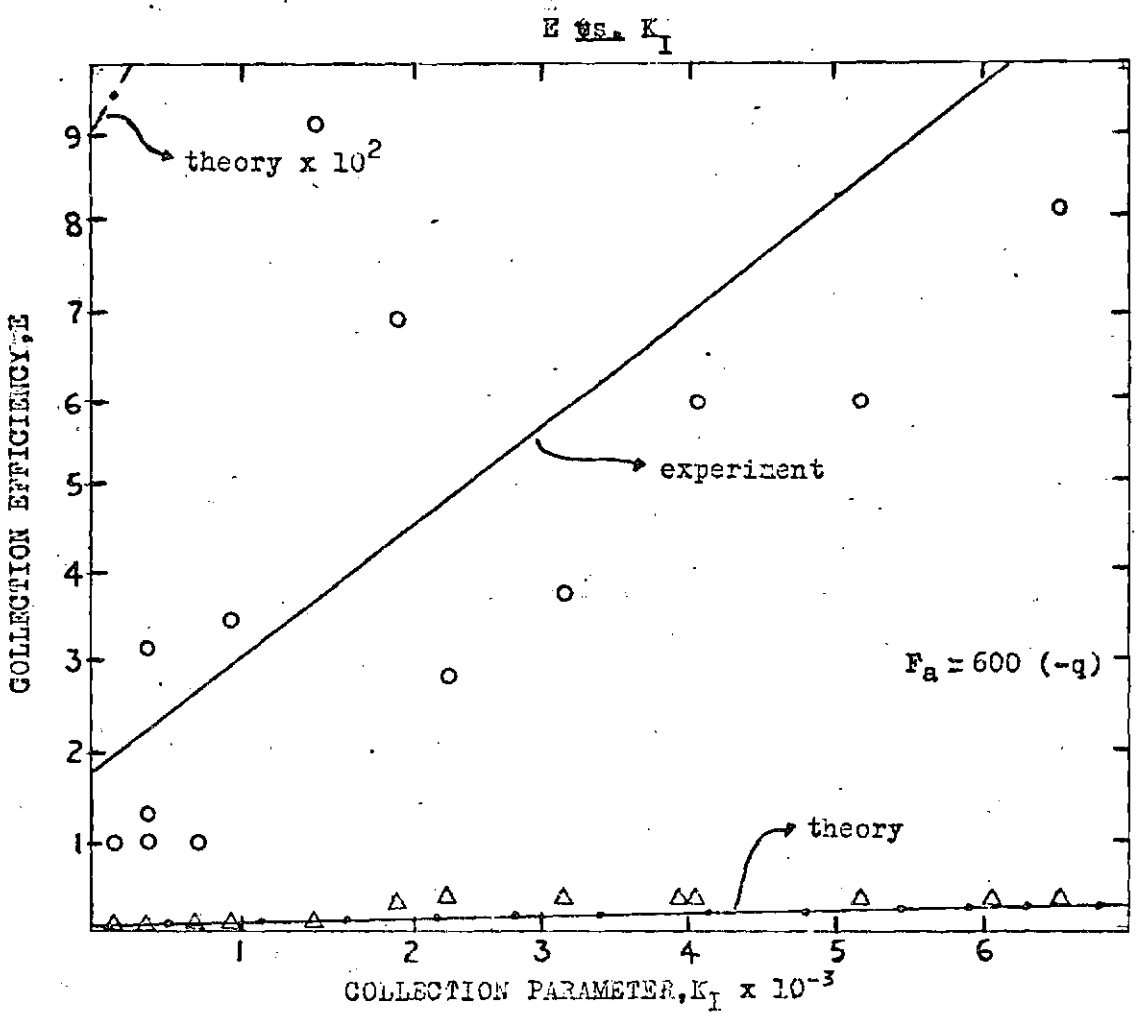

Figure 9a. Graph of Efficiency vs. Collection Parameter

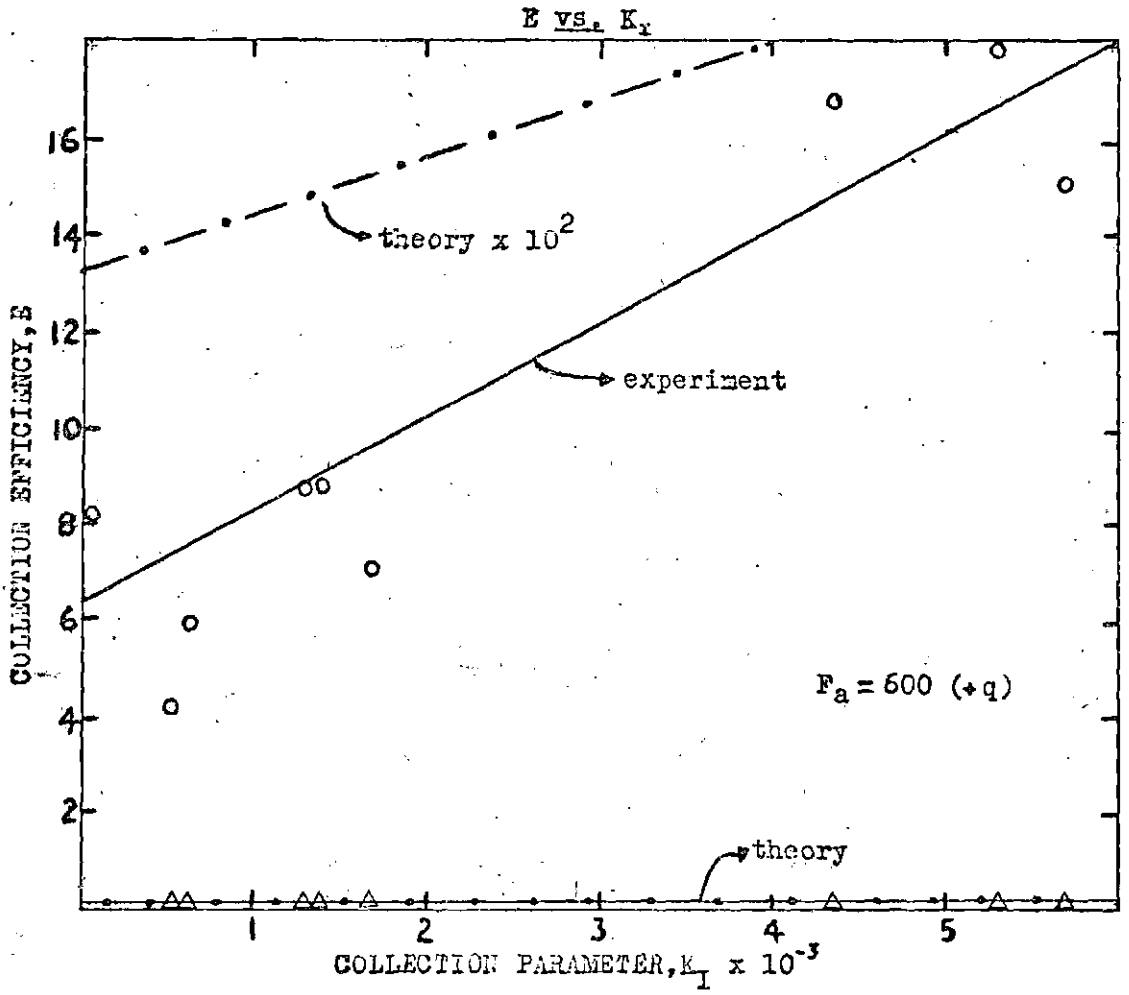

Figure 9b. Graph of Efficiency vs. Collection Parameter

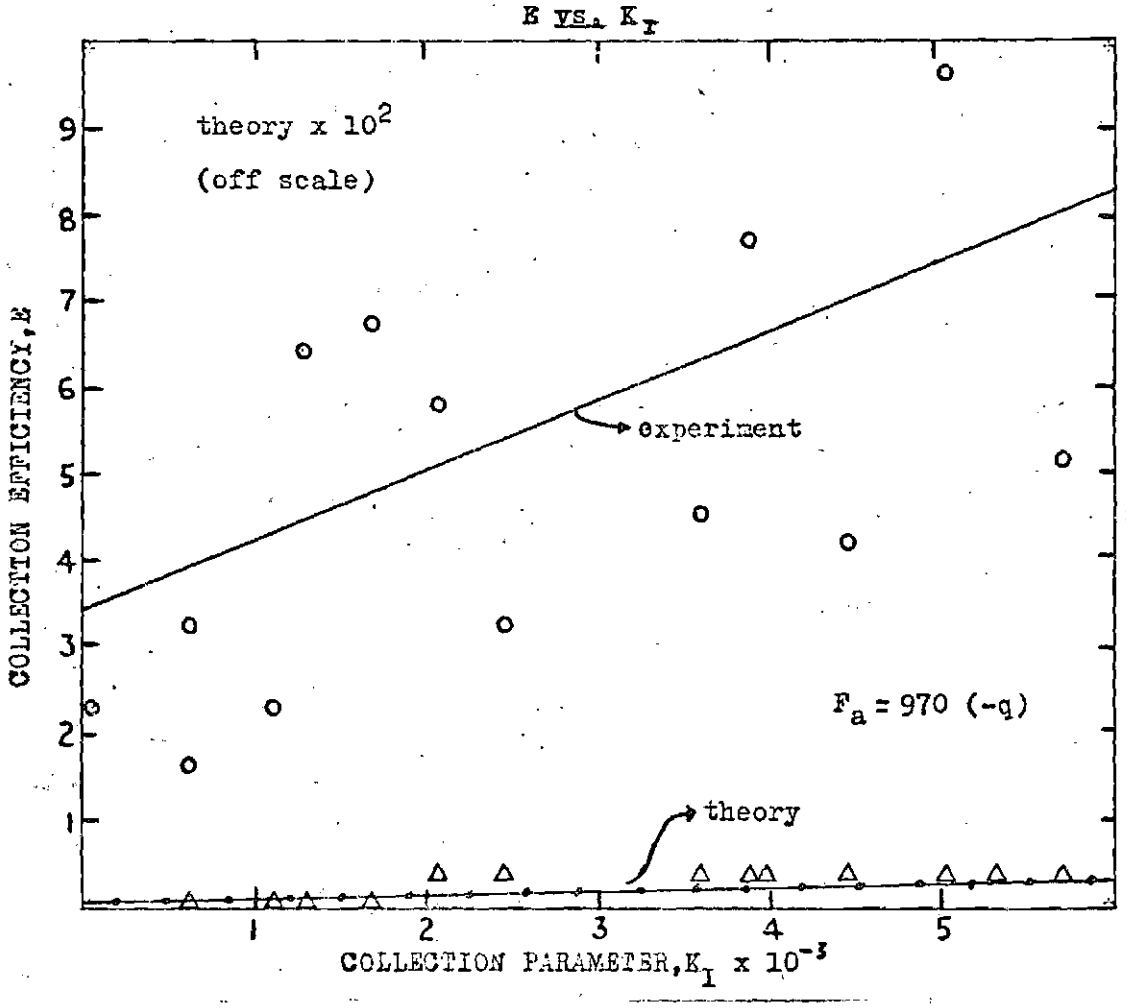

Figure 10a. Graph of Efficiency vs. Collection Parameter

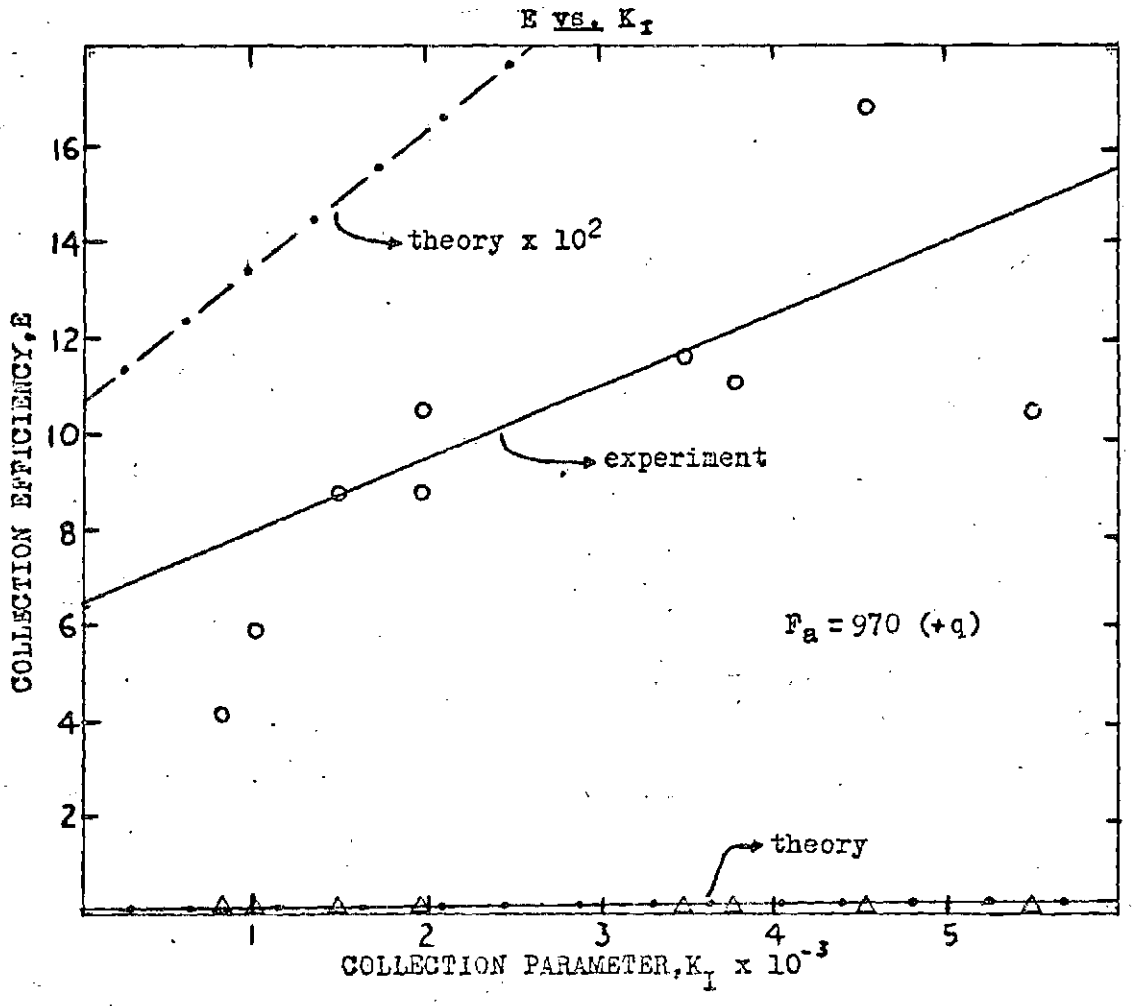

Figure 10b. Graph of Efficiency vs. Collection Parameter

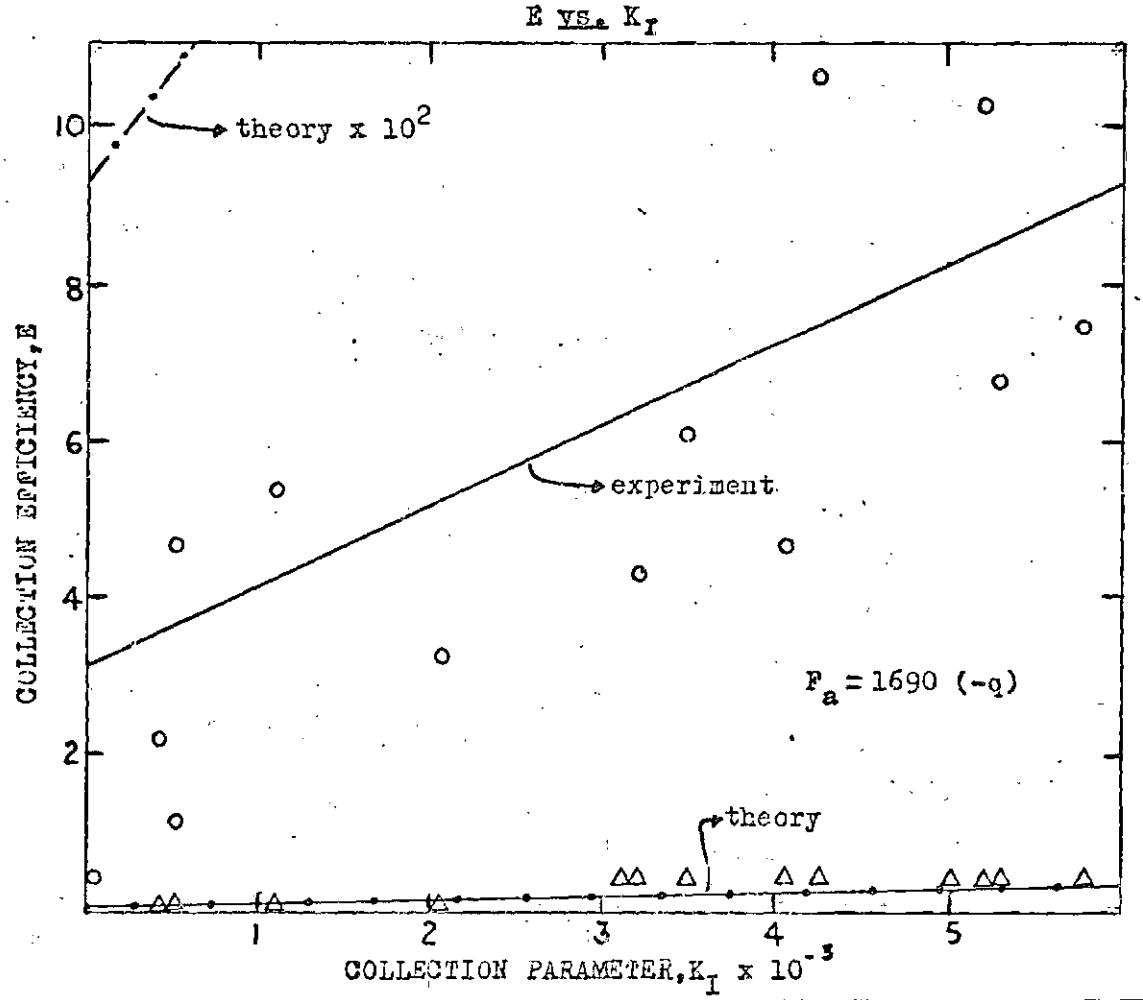

Figure 11a. Graph of Efficiency vs. Collection Parameter

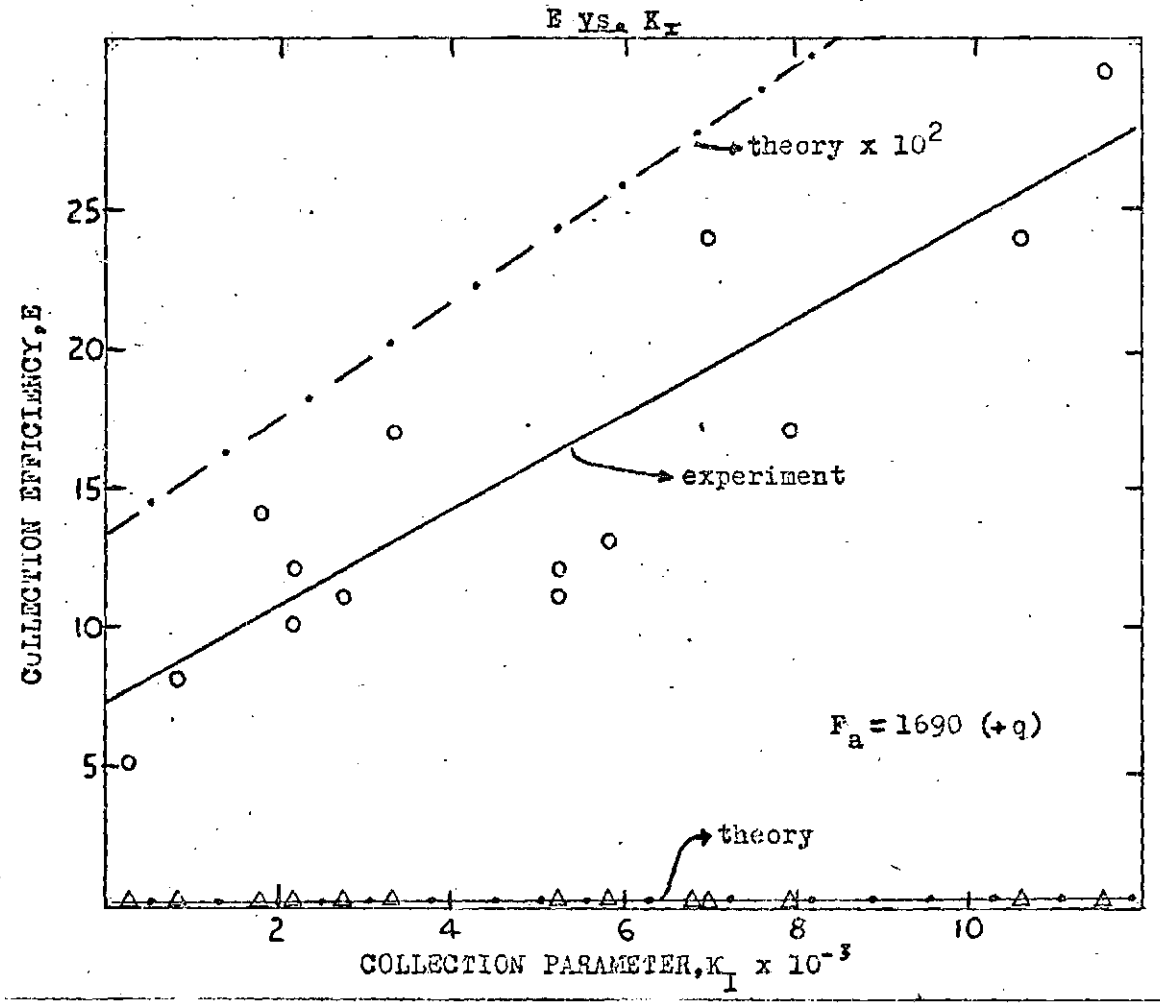

Figure 11b. Graph of Efficiency vs. Collection Parameter

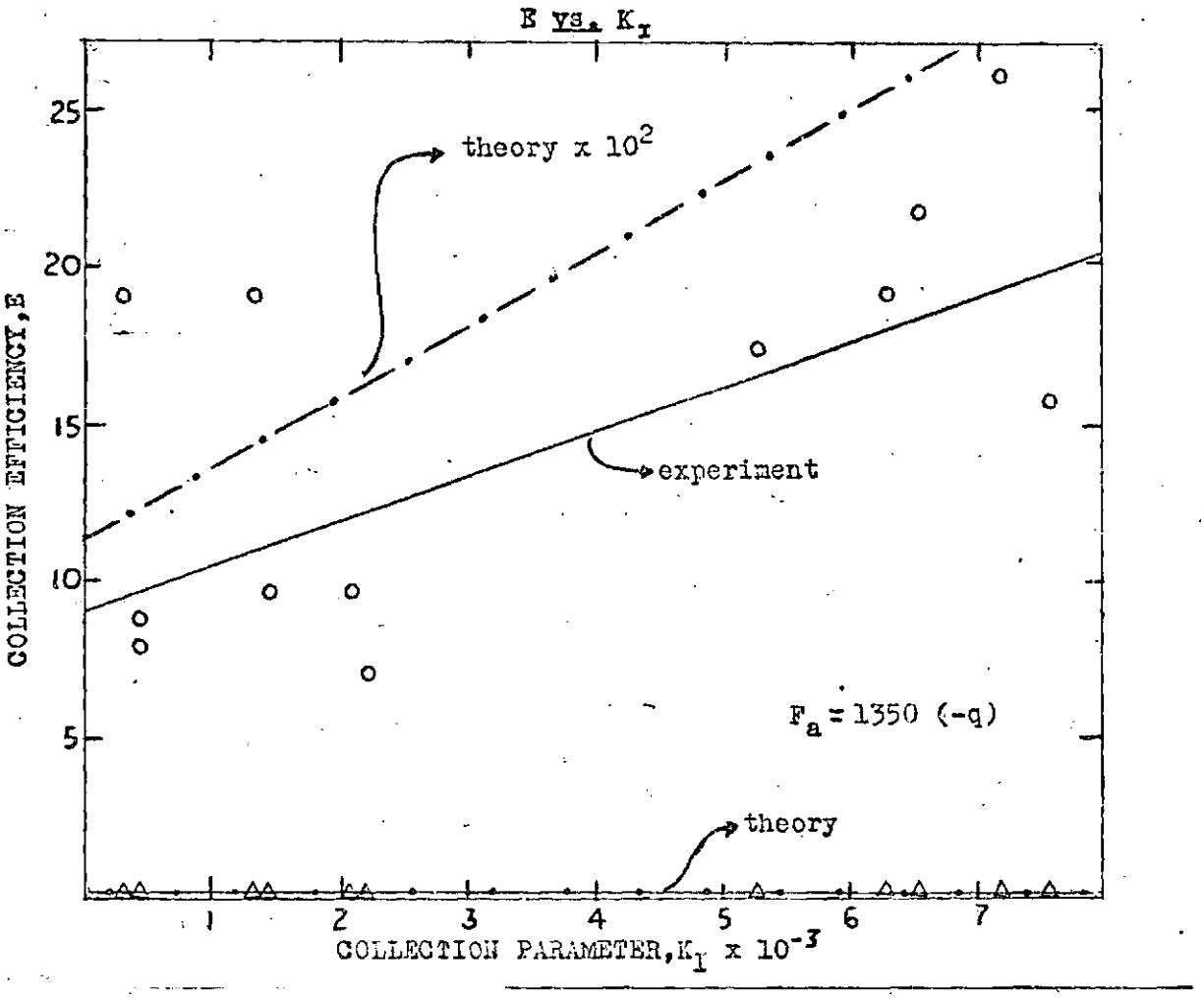

Figure 12a. Graph of Efficiency vs. Collection Parameter

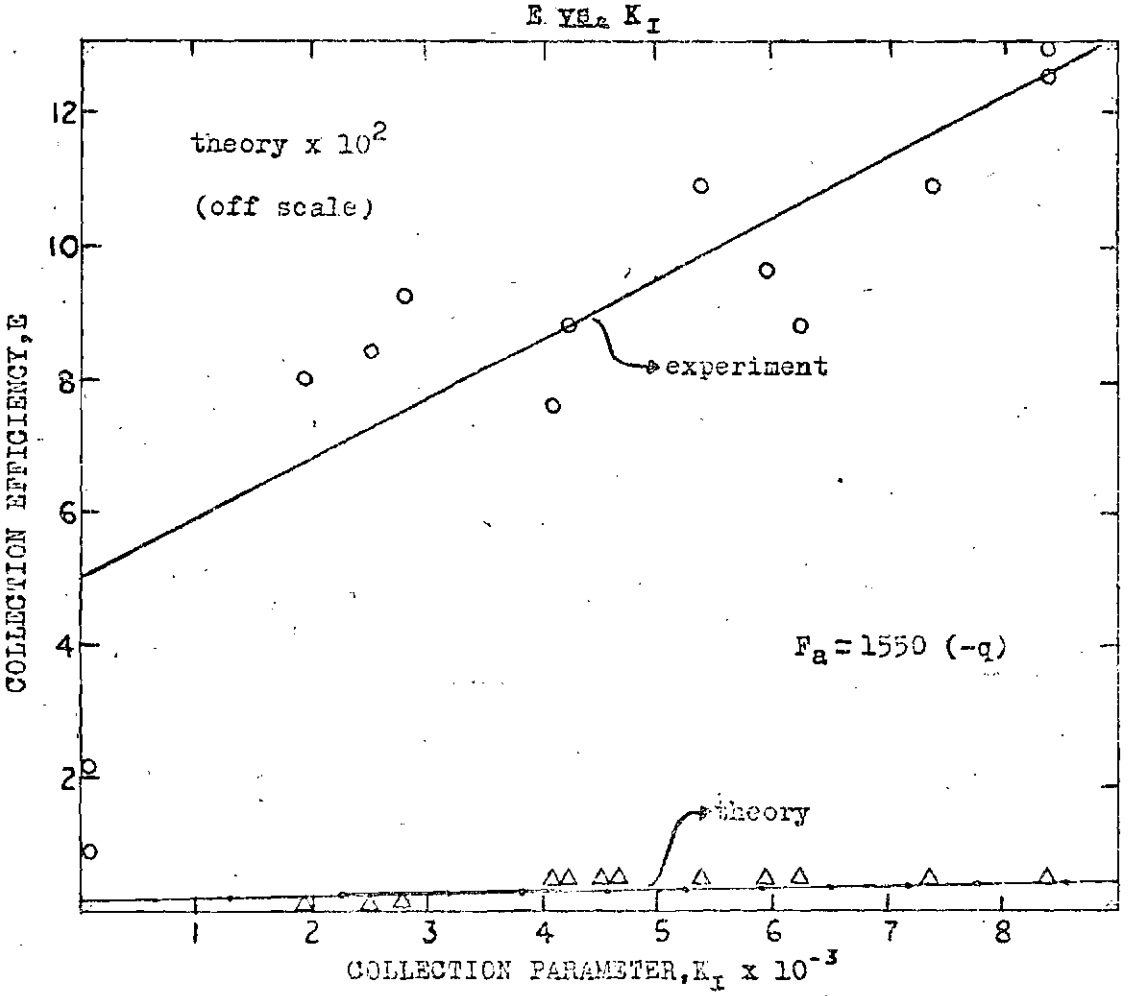

Figure 12b. Graph of Efficiency vs. Collection Parameter

CHAPTER V

CONCLUSIONS

In light of the preceding results, the following conclusions may be drawn:

1. The deposition of aerosol particles increased with the surface charge density of the water droplets. The exact relationship, however, was not determined.

2. The deposition of aerosol on positive charged water droplets was greater than that on negative charged droplets. This effect was observed because the aerosol contained a greater amount of negative charge carriers than positive ones.

3. The theory of Kraemer and Johnstone may be used to approximate the collection efficiency of naturally charged aerosol particles on charged water droplets.

4. The water in the reservoir above the needle was left with a positive charge after the needle had been subjected to high voltage of either polarity.

CHAPTER VI

RECOMMENDATIONS

The results of this study show the increased effectiveness of water as a particulate scavenging agent when it carries a surface charge. More study should be done to investigate this phenomenon more thoroughly. There are several improvements that should be made to guarantee more realiable data. An optimum drop source is needed and some work on the effect of capillary size would be fruitful. Aerosols of larger size particles should be tested and improvements made in the set-up to assure no deposition of aerosol on the water being collected in the collector. Careful measurements of the important collection parameters and the collection efficiences should be made, and the theory of Kraemer and Johnstone thoroughly tested. More work in this area is recommended.

APPENDIX

APPENDIX 1

CONSTRUCTION, FUNCTIONS AND CALIBRATION OF THE FLUOROMETER

The Turner, Model 111, fluorometer is based on the concept of an optical bridge which is analogous to the accurate Wheatstone bridge used in measuring electrical resistance. This bridge detects the difference between the light emitted by the sample and the light of a rear light path (see Figure 13). The same source is used to excite the sample and to furnish light for the rear light path so that differences in light source output will be compensated since both will vary the same. The forward light path allows light to always hit the photomultiplier tube even if there is no sample in place. This allows one to set the instrument at zero and thus measure the fluorescence of a blank. A light interrupter alternately allows light from the sample and light from the rear light path to hit the photomultiplier. The blank knob sets the rear light path equal to the fluorescence of a convenient standard (blank or other). The light cam which is attached to the fluorescence dial is turned by means of a servo motor until the light in the rear light path balances or equals that light emitted from the sample. Each dial division adds equal increments of light to the rear light path. When the two light paths are balanced, the amount of fluorescence is indicated from the dial reading.

The fluorometer comes equipped with several cuvets which serve as liquid sample holders. Since any type of foreign material, even

fingerprints, may give a fluorescence reading, the cuvets were washed thoroughly with laboratory detergent and dried with Kim wipes. Each cuvet, in turn, was then placed in the fluorometer and its reading recorded. Each one gave a very low reading (<5) and fell within 1 unit division of each other. The fluorescence dial is composed of 100 divisions. This procedure assured that no discrepacy would result from use of different cuvets. Next, several cuvets were filled with distilled water and placed in the fluorometer. The dial was set at zero for the first sample and checked with the other samples. There was no appreciable change. Upon completion of this task, several aqueous solutions of sodium chloride (NaCl) and uranine, as a tracer, were made from which the aerosol was generated. A 1% solution was made first, the concentration being 0.9% NaCl and 0.1% uranine, i.e., 1% solute by weight. This solution was then diluted to form a 0.1% solution. The procedure continued, diluting by one tenth each time, until solutions down to 10^{-6}% were obtained. The 0.1% solution made from the 1% solution was checked by making an original 0.1% solution. Two cuvets of each solution made were placed in the fluorometer and readings recorded. The recorded values were plotted on logarithmic graph paper and showed a linear relationship between the concentration of solute and the dial reading. The readings for the two 0.1% solutions agreeded very closely. This plot, shown in Figure 14, thus served as a calibration curve for the fluorometer in determining the concentration of the solute in distilled water samples. The cuvets were washed after each use and were wiped with Kim wipes before being inserted into the fluorometer. The small beakers used to transport

the samples were also washed after each use.

The fluorometer was also accompanied by several filters which transmit only certain wavelengths of light favorably. In addition to these filters, there were several neutral density filters which served as attenuators. At least two filters had to be used at any one time, a primary filter and a secondary filter. The primary filter was placed between the sample and light source and was used to isolate a specific spectral region of the light source. The secondary filter was placed between the sample and photomultiplier tube and allowed only light from the sample to pass through to the photodetector. One or more neutral density filters often accompanied the secondary filter. When using the different filters, the blank (pure distilled water sample) reading had to be set at zero for each set of filters. All samples from this experiment were measured using the same set of filters, with the exception of the neutral density filters.

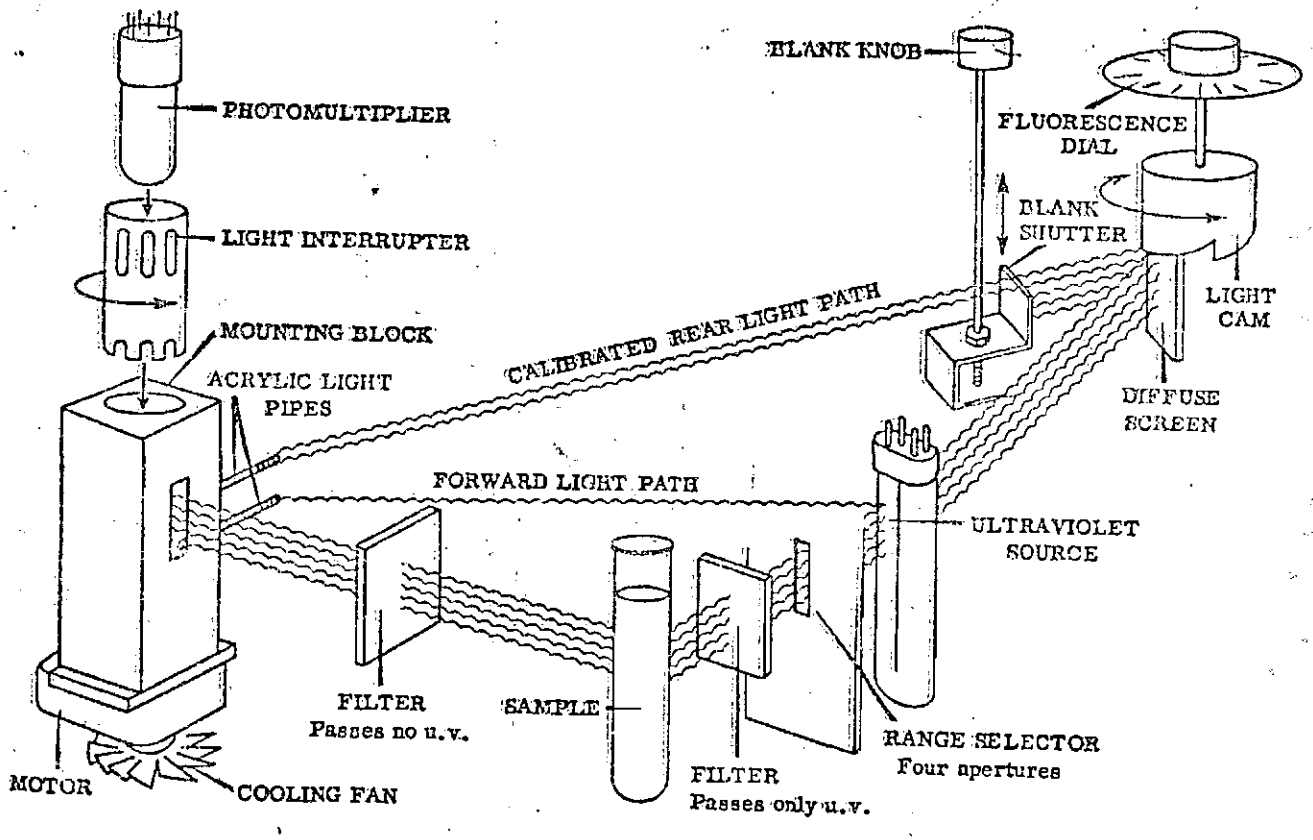

Figure 13. Optical Design of the Fluorometer

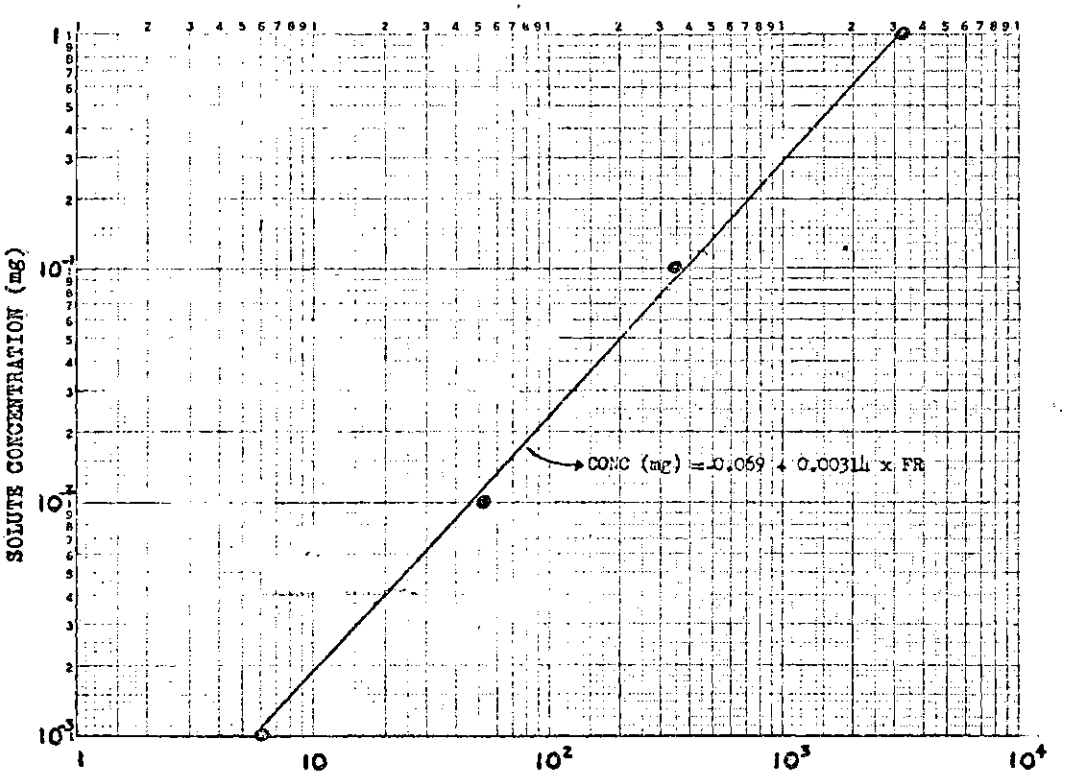

Figure 14. Calibration Curve for the Fluorometer

APPENDIX 2

AEROSOL CHARACTERIZATION

The generated aerosol for this study was characterized by collecting the aerosol particles on an electron microscope grid and then determining the necessary parameters from a microphotograph.

The aerosol was generated from a 1% aqueous solution of NaCl and uranine by the method discussed in Chapter II. The generated aerosol flowed into the dryer at 14 liters/min. (20 psi) while dry air was pumped in at 12 liters/min. The fine, dry aerosol stream which left the dryer was then mass analyzed. To determine the mass density of the aerosol stream, a 0.1 ft^3 sample of it was passed through a Millipore filter and a wet test meter. The filter was removed, carefully washed in a sample of water, diluted to 50 ml, and analyzed with the fluorometer. The reading obtained was easily related to the total mass of aerosol in any given volume of the aerosol stream. It was found that the No. 40 DeVilbiss nebulizer gave a mass concentration of 1220 mg/cm^3.

Besides knowing the mass density of the aerosol, a size distribution was also needed. To determine the size distribution of the particles, the aerosol was allowed to pass through a device containing two electrodes, between which the aerosol flowed. One of these electrodes held an electron microscope grid on its tip. This device is commonly called an electrostatic precipitator. As the stream passed between the two electrodes a high potential was applied between the

two electrodes causing the aerosol particles to precipitate onto the grid. The grid was then removed and photographed with an electron microscope assembly, the magnification being 9900x. Size analysis was then made using this photograph (see Figure 15) and a Zeiss T6Z3 particle counter. This type counter contained an area diaphragm located between a light source and a lighted screen on which the photograph rested. The area diaphragm allowed a circular spot of light of variable diameter to be projected onto the photograph. The area of the spot of light was then varied until it corresponded closely to the particle size on the photograph. At this point a switch was released which marked the particle of interest by punching a hole in it and at the same time incremented by one unit a scaler which corresponded to the particular size of the light spot and hence to the particle of interest. There were fifty such counters each corresponding to a known size range. All of the particles on the photograph were counted but some were too small to be measured by the particle counter. For the DeVilbiss nebulizer there were 198 particles too small to be counted compared with 394 in the applicable range.

After completion of a measurement the values of the individual scalers and of the summation scaler are noted. These readings, however, had to be multiplied by a correction factor to obtain correct x-values of the distribution curve with exponentially increasing step widths. This procedure was necessary because the diameter of the measuring spot of light increased exponentially with the counter number. Upon completion of this task, a percent cumulative frequency was calculated for each size range or scaler value and plotted on log

probability paper against the midpoint of its range. For a normal distribution this plot would be linear with the diameter at 50% cumulative frequency being the geometric mean. The geometric standard deviation would be found from such a plot by dividing the value of the diameter at 84.13% by that at 50%. The plot for the present data, however, could be best described as two intersecting straight lines (see Figure 16). Such a plot indicated that the aerosol was composed of two distinct distribution of particles, i.e., a bi-normal distribution. This occurrence did not come as a surprise for it is a well known fact that when liquids are separated into droplets at high rates, a thin filament is drawn between the separating elements. This filament finally breaks away from the droplets and forms a much smaller droplet known as a satellite droplet. It is suggested then that the two distributions of particles found in this study resulted from this phenomenon.

Quantitative data could not be obtained from the plot in its original form. Nevertheless, by separating the points into two groups, the needed parameters were obtained. Groups were formed by placing those points that followed the first straight line into one group and those that followed the other line in a second group (see Figures 17, 18). From these two plots, the geometric mean and standard deviation were determined. The position of the geometric means for the two size distributions cannot be clearly seen in a plot like Figure 16. On the other hand, a plot of frequency against the logarithm of the particle diameter shows clearly the position of these points (Figure 19).

The aerosol characteristics determined from this analysis are summarized in Table 1 below.

Table 1. Mass and Size Distribution of Aerosol

Group 1 Large Particles

geometric mean diameter D_g = 0.106 μm

geometric standard deviation σ_g = 2.33

Group 2 Small Particles

geometric mean diameter D_g = 0.093 μm

geometric standard deviation σ_g = 1.06

Mass Concentration = 1220 mg/cm^3

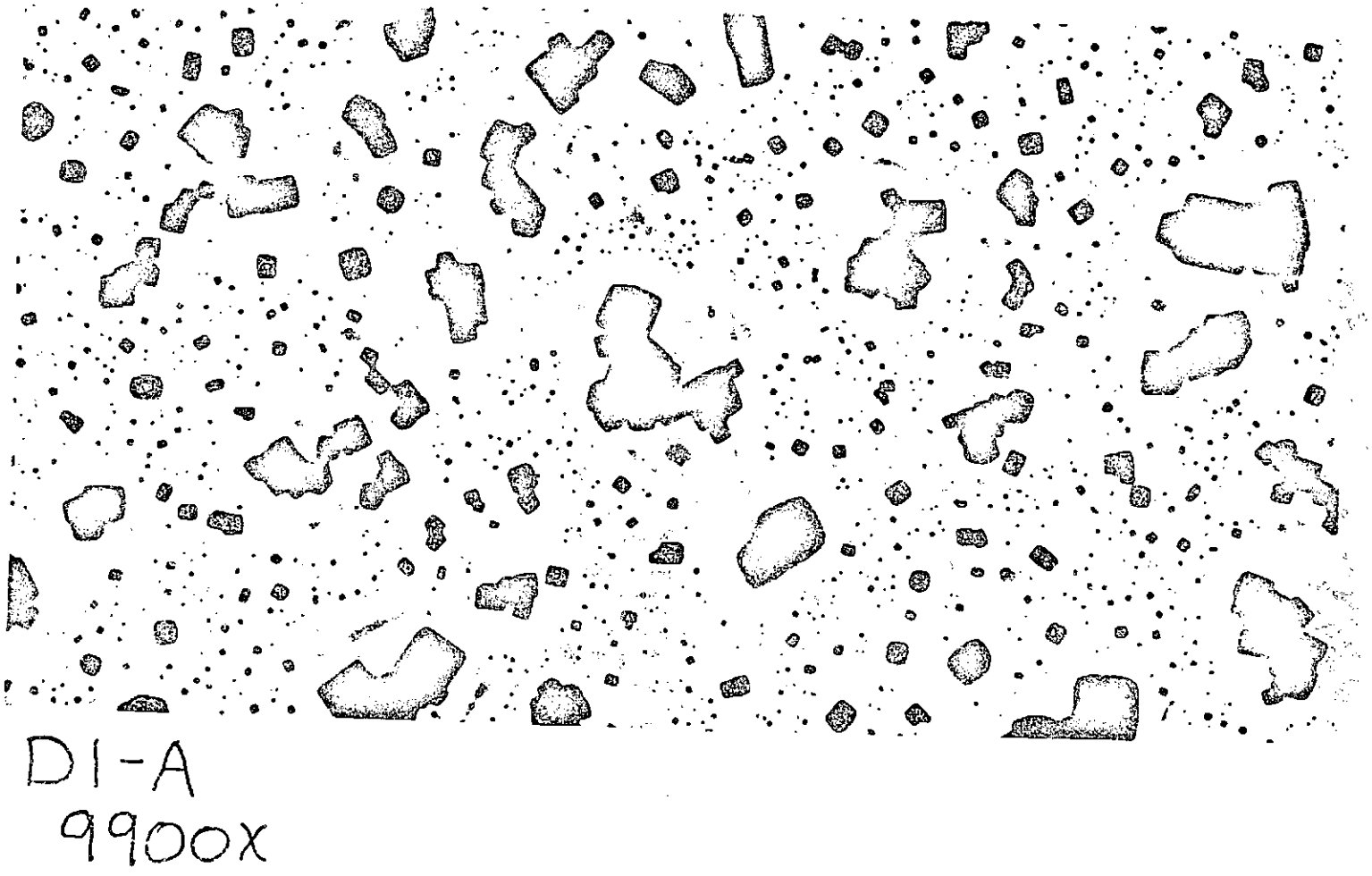

Figure 15. An Example of a Micro-Photograph

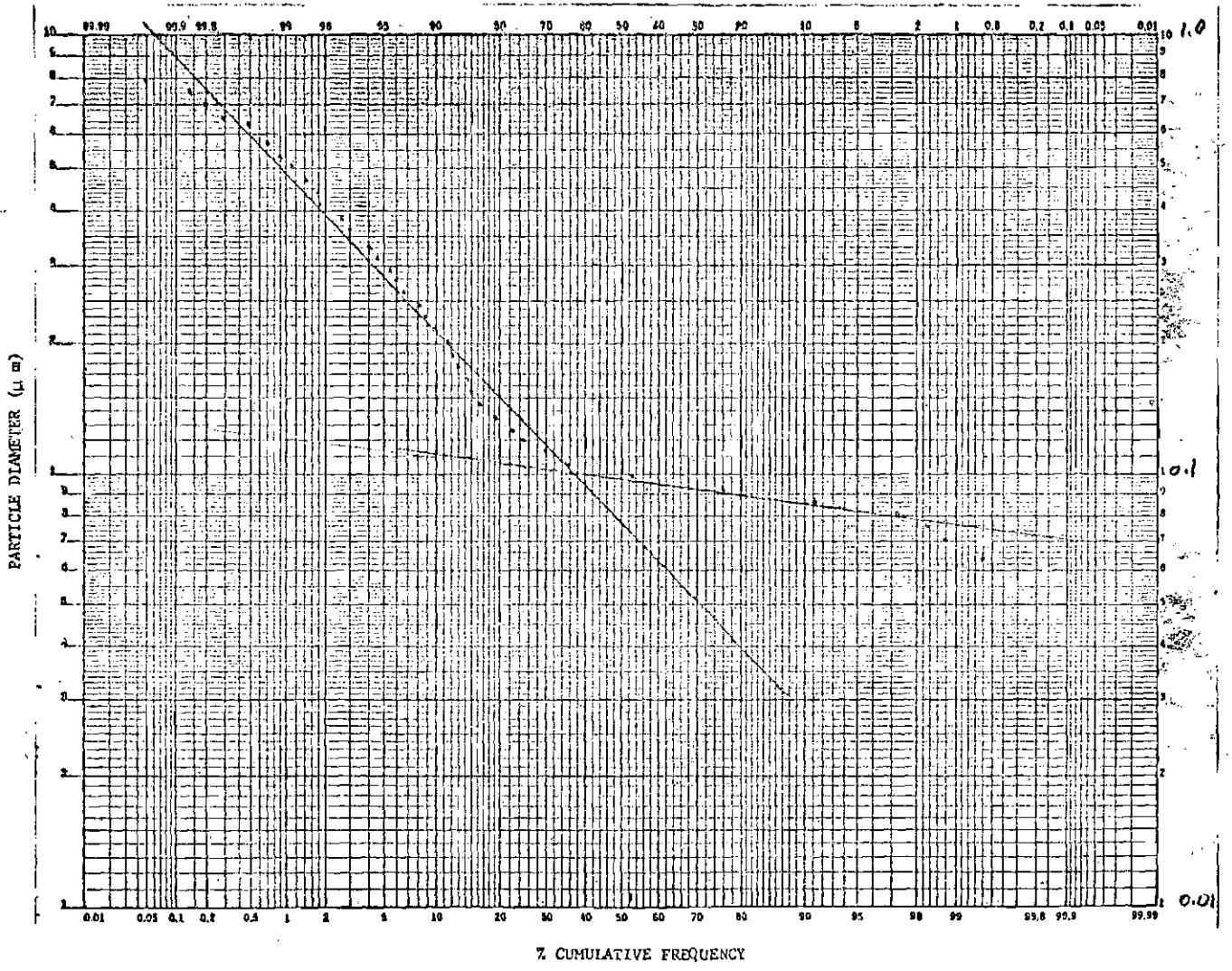

Figure 16. Size Distribution of All Aerosol Particles

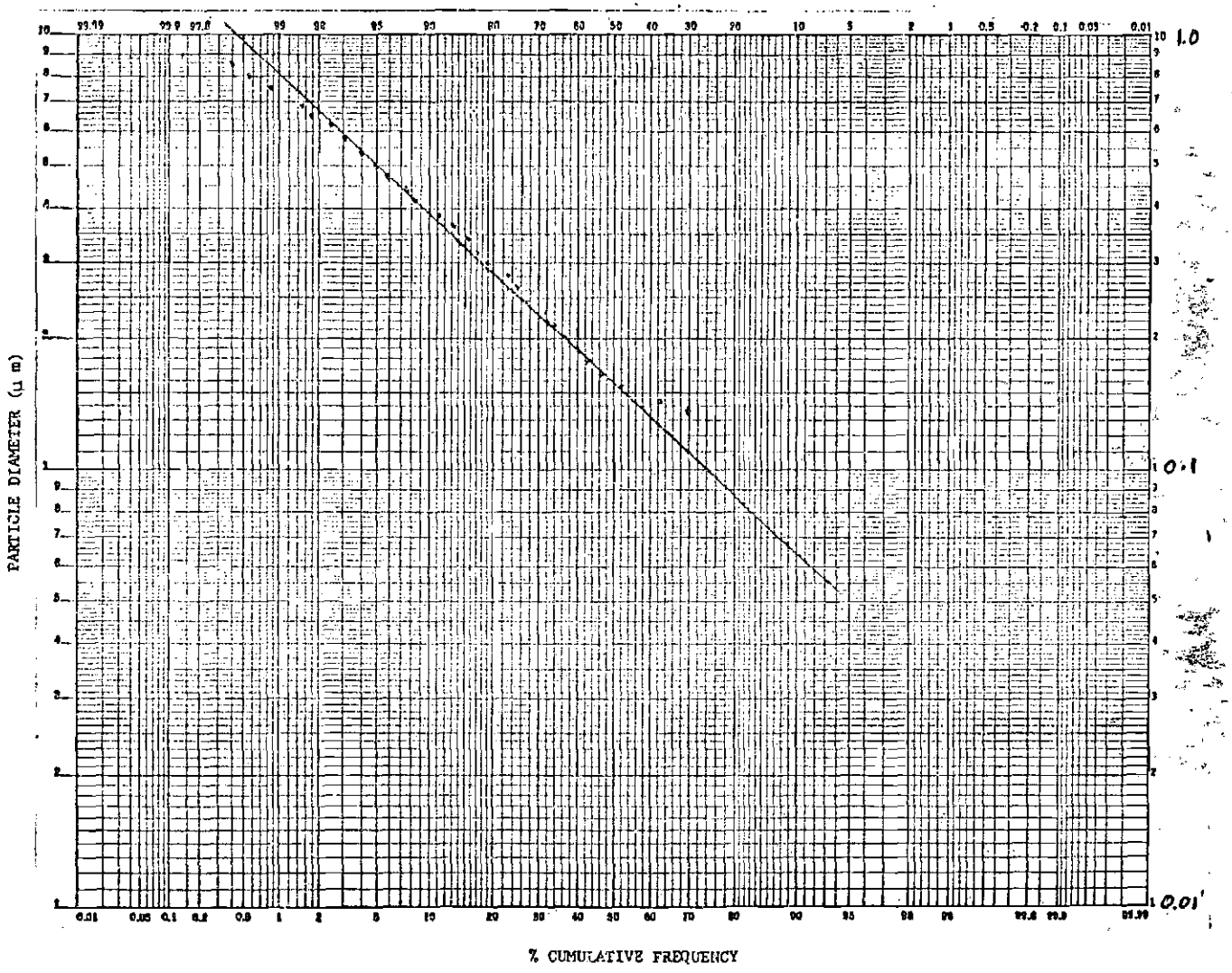

Figure 17. Size Distribution of Large Aerosol Particles

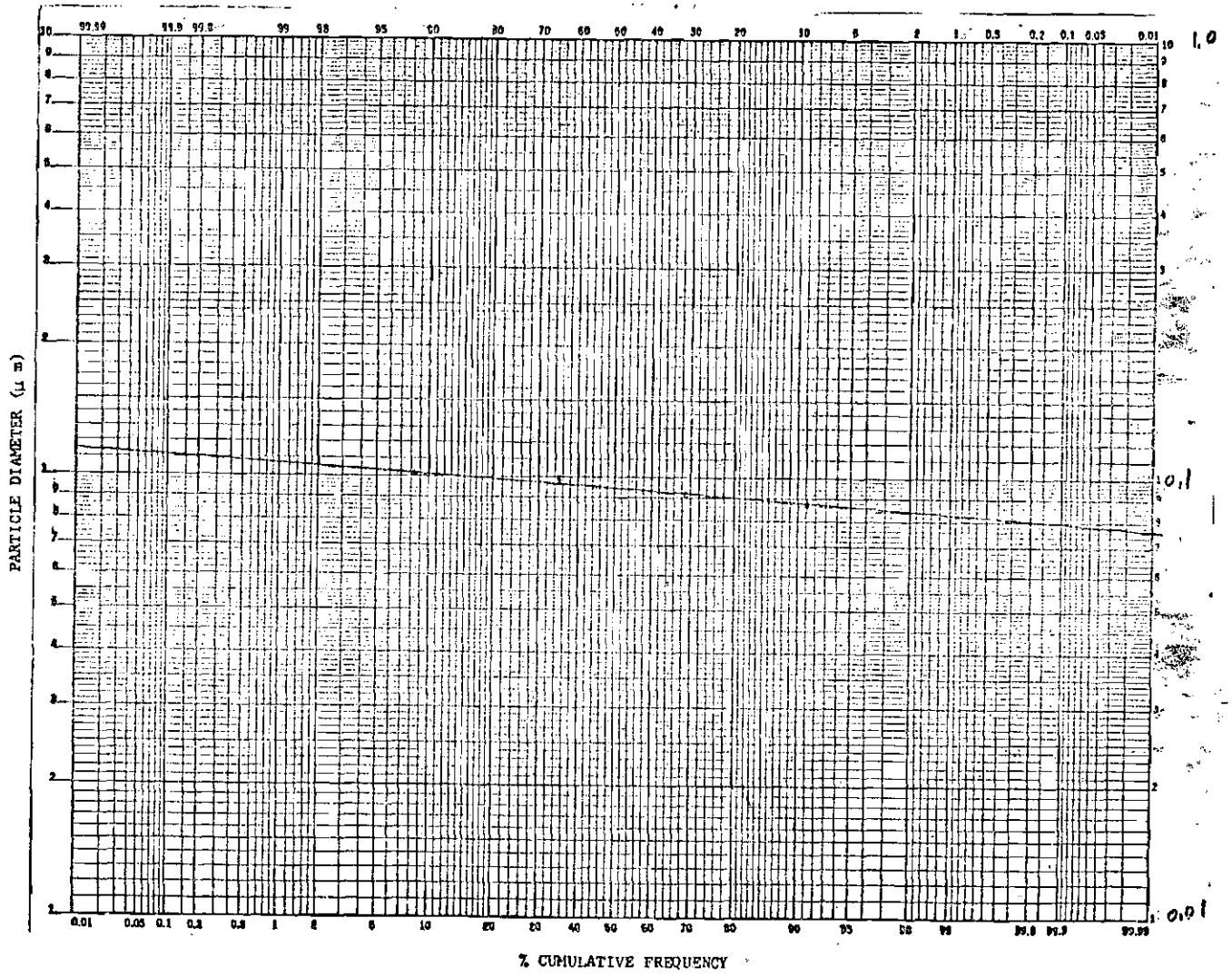

Figure 18. Size Distribution of Small Aerosol Particles

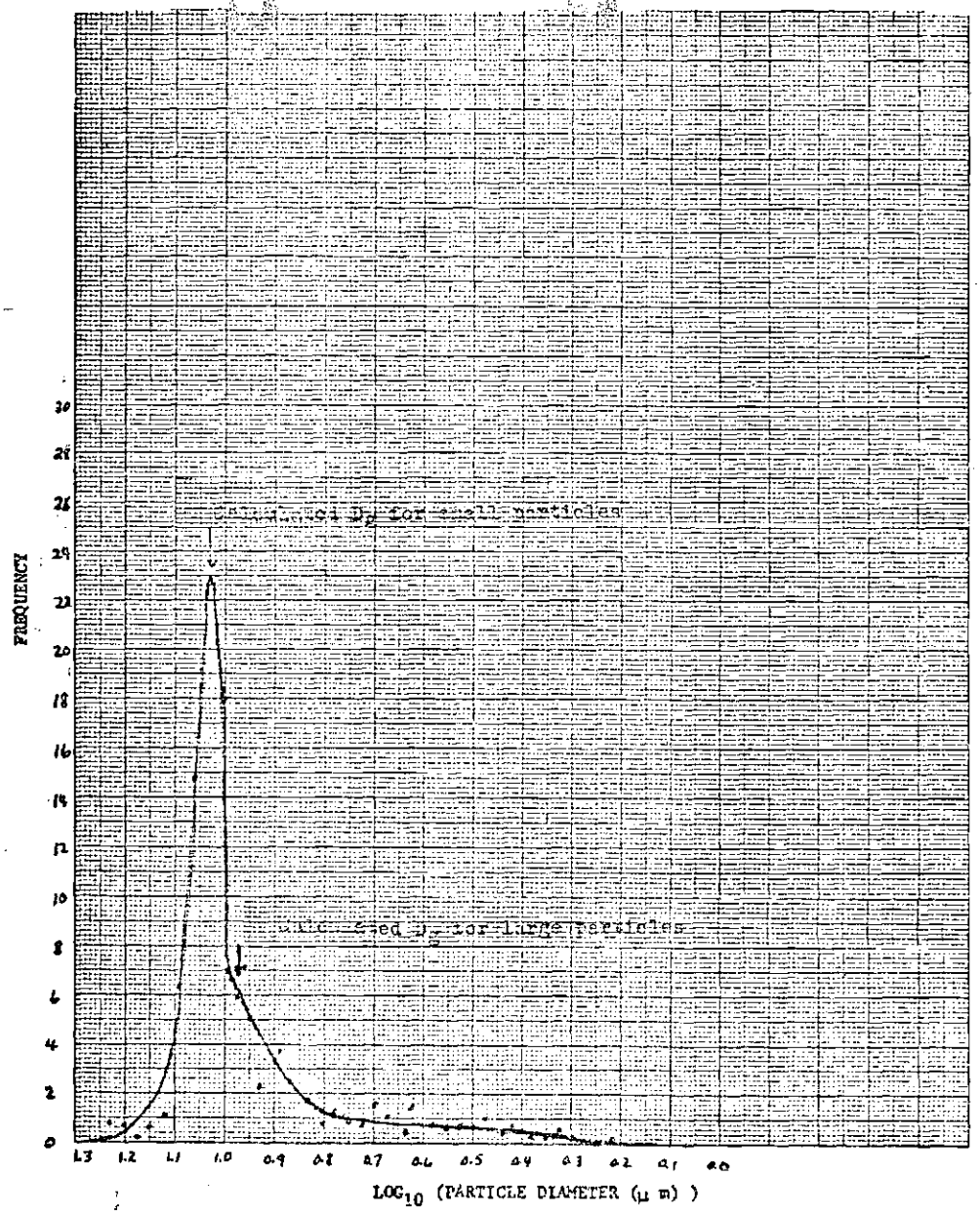

Figure 19. Frequency Distribution of Aerosol Particles

APPENDIX 3

DERIVATION OF THE CAPACITOR CHARGING CURVE - EQUATION 5

The current, Q_0, now called I_0, was calculated using the voltage and charge relationship for the capacitor, namely,

$$V = Q/C = I_1 R_s$$

where R_s is the system resistance and I_1 is the leakage current.

$$\frac{dV}{dt} = \frac{(dQ/dt)}{C}$$

$$\frac{dQ}{dt} = I_0 - I_1 = I_0 - V/R_s$$

Separating variables and integrating gives

$$\frac{1}{R_s C}\int_{t_o}^{t_c} dt = \int_{V_o}^{V_c} \frac{dV}{I_0 R_s - V}$$

$$-(t_c - t_o)/R_s C = \ln(I_0 R_s - V_c) - \ln(I_0 R_s - V_o)$$

Choosing $t_o = V_o = 0$ yields

$$-\frac{t_c}{R_s C} = \ln\left(\frac{I_0 R_s - V_c}{I_0 R_s}\right) = \ln(1 - V_c/I_0 R_s)$$

$$\exp(-t_c/R_sC) = 1 - V_c/I_0R_s$$

and thus

$$I_0 = \frac{V_c}{R_s}\left[1 - \exp\left(-\frac{t_c}{R_sC}\right)\right]^{-1}$$

Substituting Q_0 for I_0 yields Equation 4

$$Q_0 = \frac{V_c}{R_s}\left[1 - \exp\left(-\frac{t_c}{R_sC}\right)\right]^{-1}$$

APPENDIX 4

EXPERIMENTALLY MEASURED PARAMETERS

Table 2. Nomenclature

A	cross-sectional area of needle's tip (cm^2)
C	Cunningham factor
C_a	amount of aerosol collected per unit area ($\mu g/cm^2$)
C_e	electrical capacitance (farads)
D_g	geometric mean diameter (μm)
σ_g	geometric standard deviation
DR	drop rate (sec^{-1})
ϵ_o	permittivity of free space = 8.85×10^{-21} $C^2/dyne\text{-}cm^2$
E	collection efficiency
F_a	volumetric flow rate of aerosol stream (cc/min)
F_f	volumetric flow rate of flushing air (cc/min)
F_w	volumetric flow rate of water (cc/min)
FR	fluorescence dial reading
K_E	collection parameter for charged aerosol on charged sphere
K_G	collection parameter for charged aerosol on grounded sphere
K_I	collection parameter for uncharged aerosol on charged sphere
N	viscosity (poises)
NOD	number of drops in collected sample
Q	total charge on each droplet (coulombs)
Q_0	current delivered to the capacitor (coulombs/min)
q	surface charge density ($coulombs/cm^2$)
r	radius of aerosol particle (μm)
R	radius of mature water droplet (mm)

Table 2. Continued

R_s	system resistance (ohms)
t_c	capacitor charging time (min)
U_0	aerosol velocity (cm/sec)
V_c	voltage across capacitor at time t_c (volts)
Vol	volume of droplet (cc)
X_s	dielectric constant of droplet

Table 3. Experimentally Measured Parameters

Run No.	F_f	F_a	F_w	DR	V_o	VR	FR
1 - 20	Void	F_a = 600 U_o^* = 5.56					
21	7600	600	1.20	76.26	-2020	3.036	120
22	7600	600	1.22	127.62	-3000	6.348	200
23	7600	600	1.22	90.36	-1495	1.860	135
24	7600	600	1.22	107.10	-2480	3.912	250
25	7600	600	1.20	87.84	-1020	0.816	60
26	7600	600	1.22	111.30	-2490	4.758	100
27	7600	600	1.33	148.50	-1900	4.578	120
28	7600	600	1.21	151.08	-2980	6.690	110
29	7600	600	1.21	112.14	-1500	1.986	70
30	7600	600	1.21	126.42	-2480	4.476	75
31	7600	600	1.21	109.68	-1010	0.846	35
32	7600	600	1.21	110.46	0	1.290	35
33	7600	600	1.21	112.14	-1010	1.206	40
34	7600	600	1.21	123.42	-2000	3.726	60
35	7600	600	1.21	112.98	0	1.776	35
			+ Volts				
36	7600	600	.880	62.04	0	0	120
37	7600	600	.865	62.16	+1020	1.026	130
38	7600	600	.855	67.62	+2010	2.280	245

* U_o here refers to the aerosol stream velocity

Table 3. Continued

Run No.	F_f	F_a	F_w	DR	V_o	VR	FR
39	7600	600	.830	73.80	+3020	3.162	375
40	7600	600	0.880	76.74	+3020	3.024	215
41	7600	600	0.880	65.64	+1475	1.068	130
42	7600	600	0.880	66.48	+1485	1.242	110
43	7600	600	0.880	73.56	+2480	2.346	235
44	7600	600	0.880	64.08	+1030	0.612	70
45	7600	600	0.880	63.72	+1030	0.678	90
		F_a = 970	U_o = 8.989				
46	7600	970	1.33	117.18	-2000	4.482	190
47	7600	970	1.33	153.42	-3000	7.782	205
48	7600	970	1.33	142.80	-3000	10.950	195
49	7600	970	1.26	95.82	-1510	2.136	105
50	7600	970	1.22	111.72	-2520	4.710	150
51	7600	970	1.18	88.62	-1000	1.146	60
52	7600	970	1.18	98.82	-2020	3.456	120
53	7600	970	1.22	132.42	-1450	3.042	110
54	7600	970	1.48	113.40	0	0	50
55	7600	970	1.15	87.42	0	0	50
56	7600	970	1.15	132.48	-2975	5.760	80
57	7600	970	1.15	88.74	-1000	1.182	40
58	7600	970	1.15	96.72	-1960	2.646	75
59	7600	970	1.15	87.06	- 525	0.192	50

Table 3. Continued

Run No.	F_f	F_a	F_w	DR	V_o	VR	FR
60	7600	970	1.15	104.16	-2470	3.600	80
61	7600	970	1.15	90.18	-1490	1.548	50
62	7600	970	1.15	108.30	-2950	4.806	90
63	7600	970	1.15	93.42	-2020	2.322	95
			+ Volts				
64	7600	970	0.800	55.44	+1030	0.708	90
65	7600	970	0.815	58.74	+1030	0.702	70
66	7600	970	0.815	62.76	+2030	1.722	160
67	7600	970	0.780	57.48	+2000	1.440	160
68	7600	970	0.815	72.96	+2995	3.000	275
69	7600	970	0.800	57.84	+1530	1.092	145
70	7600	970	0.815	59.58	+1530	1.146	130
71	7600	970	0.815	59.34	+1500	0.972	130
72	7600	970	0.815	66.84	+2530	2.298	150
73	7600	970	0.815	65.76	+2505	2.028	235
74	7600	970	0.815	71.82	+2990	2.904	180
		F_a = 1690	U_o = 15.66				
75	7600	1690	1.14	155.16	+3030	7.908	195
76	7600	1690	1.14	141.48	+3030	7.170	205
77	7600	1690	0.58	39.48	+1020	0.588	190
78	7600	1690	0.94	73.08	+1020	1.038	125
79	7600	1690	1.22	131.28	+2040	4.002	165

Table 3. Continued

Run No.	F_f	F_a	F_w	DR	V_o	VR	FR
80	7600	1690	1.00	98.76	+2040	4.008	170
			- Volts				
81	7600	1690	1.10	99.00	-2490	4.050	110
82	7600	1690	1.13	87.84	-1495	2.106	60
83	7600	1690	1.13	121.68	-2985	5.748	125
84	7600	1690	1.13	91.86	-2000	3.180	80
85	7600	1690	1.13	84.24	-1000	0.930	35
86	7600	1690	1.13	96.30	-1990	3.018	75
87	7600	1690	1.05	81.36	0	0.120	25
88	7600	1690	1.05	94.02	-1990	3.042	100
89	7600	1690	1.05	107.40	-2995	4.536	160
90	7600	1690	1.05	82.02	-1015	0.828	50
91	7600	1690	1.05	93.90	-2500	3.348	160
92	7600	1690	1.05	82.86	-1520	1.362	90
93	7600	1690	1.05	97.98	-3020	3.888	215
94	7600	1690	1.02	79.74	-1470	0.930	80
95	7600	1690	1.02	86.58	-2510	2.544	265
			+ Volts				
96	7600	1690	0.72	46.56	0	0.210	85
97	7600	1690	0.72	57.42	+2000	2.184	230
98	7600	1690	0.72	48.96	+1025	0.906	160
99	7600	1690	0.70	67.02	+3010	3.342	420

Table 3. Continued

Run No.	F_f	F_a	F_w	DR	V_o	VR	FR
100	7600	1690	0.72	52.62	+1520	1.248	230
101	7600	1690	0.76	66.66	+2510	2.520	725
102	7600	1690	0.72	51.60	+1500	1.080	160
103	7600	1690	0.68	61.80	+2960	2.826	330
104	7600	1690	0.66	54.12	+2520	1.866	325
		F_a = 1350	U_o = 12.51				
105	7600	1350	1.14	191.04	-3030	11.862	330
106	7600	1350	1.08	105.84	-2020	4.488	250
107	7600	1350	1.04	84.48	-1010	1.962	145
108	7600	1350	1.01	116.64	-2500	5.730	330
109	7600	1350	0.99	78.00	- 980	1.452	145
110	7600	1350	0.99	107.16	-2470	5.322	385
111	7600	1350	0.98	105.24	-2470	5.322	240
112	7600	1350	0.99	79.02	-1010	4.872	100
113	7600	1350	0.99	131.28	-2970	1.326	300
114	7600	1350	0.99	81.30	-1480	6.486	170
115	7600	1350	0.98	105.24	-2510	2.166	290
116	7600	1350	0.98	74.16	0	4.806	90
117	7600	1350	1.63	166.62	-1920	0.720	132
118	7600	1350	1.56	375.00	-2860	7.920	185
119	7600	1350	1.56	206.88	-2390	16.710	190
120	7600	1350	0.48	133.02	-1440	10.416	150

Table 3. Continued

Run No.	F_f	F_a	F_w	DR	V_o	VR	FR
121	7600	1350	1.20	141.84	-1950	4.482	120
		F_a = 1550	U_o = 14.36				
122	7600	1550	0.88	68.76	- 980	2.772	155
123	7600	1550	1.05	115.14	-2490	4.716	240
124	7600	1550	1.23	146.34	-2980	6.726	220
125	7600	1550	1.35	111.06	-2960	4.404	220
126	7600	1550	1.14	88.98	0	0	30
127	7600	1550	1.14	87.84	-1010	5.400	100
128	7600	1550	1.05	87.84	-1010	5.400	105
129	7600	1550	0.92	114.72	-3010	5.376	160
130	7600	1550	0.92	84.84	-1990	2.802	120
131	7600	1550	0.92	97.86	-2510	4.290	140
132	7600	1550	0.98	81.48	-1495	2.130	130
133	7600	1550	1.40	102.00	0	0	30
134	7600	1550	1.33	177.84	-1950	5.832	140
135	7600	1550	0.88	94.38	-2000	4.716	195
136	7600	1550	0.88	94.32	-2000	4.716	200
137	7600	1550	1.14	88.92	0	0	50
138	7600	1550	1.05	80.28	-1500	2.640	130
139	7600	1550	0.92	102.18	-2495	4.830	150
140	7600	1550	0.92	121.92	-3010	5.526	180

APPENDIX 5

CALCULATED PARAMETERS

Table 4. Calculated Parameters

Run No.	Q $\times 10^{-9}$	q $\times 10^{-9}$	q^2 $\times 10^{-18}$	C_a	Vol $\times 10^{-3}$	R	NOD	K_I $\times 10^{-3}$	E	U_o
1-20		Void		F_a = 600						
21	11.65	3.53	12.52	3.210	15.73	1.554	317	6.54	8.50	27.40
22	14.56	3.17	10.06	4.921	9.55	1.316	523	6.10	13.03	27.85
23	6.02	1.65	2.73	3.509	13.50	1.477	370	1.47	9.29	27.85
24	10.69	2.61	6.85	6.698	11.39	1.395	438	3.92	17.74	27.85
25	2.71	0.75	0.56	1.188	13.66	1.482	365	0.30	3.14	27.40
26	12.51	2.98	8.91	2.262	10.96	1.377	456	5.17	5.99	27.85
27	9.02	1.88	3.54	2.657	8.95	1.287	558	2.01	7.03	30.37
28	12.96	2.50	6.29	2.298	8.00	1.240	624	4.08	6.08	27.63
29	5.18	1.22	1.49	1.386	10.79	1.370	463	0.87	3.67	27.63
30	10.36	2.25	5.10	1.468	9.57	1.317	522	3.12	3.88	27.63
31	2.25	0.54	0.29	0.380	11.03	1.380	453	0.16	1.00	27.63
32	3.41	0.81	0.66	0.377	10.95	1.377	456	0.38	1.00	27.63
33	3.14	0.74	0.55	0.521	10.79	1.370	463	0.32	1.38	27.63

Table 4. Continued

Run No.	Q x 10^{-9}	q x 10^{-9}	q^2 x 10^{-18}	C_a	Vol x 10^{-3}	R	NOD	K_I x 10^{-3}	E	U_o
34	8.83	1.95	3.83	1.062	9.80	1.327	510	2.32	2.81	27.63
35	4.60	1.08	1.16	0.374	10.71	1.367	466	0.68	0.99	27.63
				+ Volts						
36	0	0	0	3.102	14.18	1.501	352	0	8.21	20.09
37	4.83	1.35	1.82	3.394	13.91	1.491	359	1.37	8.99	19.75
38	9.87	2.59	6.71	6.772	12.64	1.445	395	5.29	17.94	19.52
39	12.54	3.04	9.27	10.32	11.24	1.389	444	7.84	27.33	18.95
40	11.10	2.66	7.08	5.604	11.03	1.380	453	5.68	14.84	20.09
41	4.76	1.30	1.69	3.352	13.40	1.473	372	1.27	8.87	20.09
42	5.46	1.48	2.19	2.718	13.23	1.467	377	1.65	7.19	20.09
43	9.33	2.36	5.57	6.364	11.96	1.418	417	4.35	16.85	20.09
44	2.79	0.77	0.60	1.501	13.73	1.485	364	0.44	3.97	20.09
45	3.11	0.86	0.75	2.125	13.81	1.489	362	0.55	5.62	20.09

Table 4. Continued

Run No.	Q x 10^{-9}	q x 10^{-9}	q^2 x 10^{-18}	C_a	Vol x 10^{-3}	R	NOD	K_I x 10^{-3}	E	U_o
				F_a = 970						
46	11.19	2.73	7.48	4.922	11.35	1.394	440	3.93	13.04	30.37
47	14.85	3.03	9.18	4.911	8.66	1.273	576	5.28	13.00	30.37
48	22.45	4.80	23.09	4.747	9.31	1.305	536	12.97	12.57	30.37
49	6.52	1.75	3.09	2.554	13.15	1.464	380	1.63	6.76	28.77
50	12.33	2.93	8.61	3.707	10.92	1.376	457	5.00	9.81	27.85
51	3.78	1.02	1.05	1.178	13.31	1.470	375	0.59	3.12	26.94
52	10.23	2.58	6.69	2.925	11.94	1.417	418	3.90	7.74	26.94
53	6.72	1.42	2.04	2.406	9.21	1.300	542	1.25	6.37	27.85
54	0	0	0	0.862	13.05	1.460	383	0	2.28	33.79
55	0	0	0	0.865	13.15	1.464	380	0	2.29	26.26
56	12.72	2.6	6.76	1.559	8.68	1.274	575	4.43	4.12	26.26
57	3.89	1.04	1.08	0.555	12.95	1.456	385	0.62	1.47	26.26
58	8.00	2.01	4.07	1.184	11.89	1.415	420	2.43	3.13	26.26

Table 4. Continued

Run No.	Q x 10^{-9}	q x 10^{-9}	q^2 x 10^{-18}	C_a	Vol x 10^{-3}	R	NOD	K_I x 10^{-3}	E	U_o
59	0.64	0.17	0.03	0.866	13.20	1.466	378	0.01	2.29	26.26
60	10.12	2.42	5.89	1.686	11.04	1.381	452	3.61	4.46	26.26
61	5.02	1.32	1.75	0.852	12.75	1.449	392	1.02	2.25	26.26
62	12.99	3.03	9.21	1.953	10.61	1.363	470	5.72	5.17	26.26
63	7.27	1.87	3.51	2.196	12.31	1.432	406	2.07	5.81	26.26
				+ Volts						
64	3.73	1.07	1.14	2.160	14.43	1.510	346	0.92	5.72	18.26
65	3.49	0.97	0.95	1.505	13.87	1.490	360	0.76	3.98	18.61
66	8.03	2.14	4.60	4.228	12.98	1.457	385	3.77	11.20	18.61
67	7.33	2.01	4.07	4.296	13.57	1.479	368	3.44	11.38	17.81
68	12.03	2.90	8.46	7.378	11.17	1.386	447	7.30	19.54	18.61
69	5.52	1.54	2.37	3.851	13.83	1.489	361	1.94	10.20	18.26
70	5.63	1.55	2.42	3.372	13.67	1.483	365	1.95	8.93	18.61
71	4.79	1.33	1.76	3.370	13.73	1.485	364	1.41	8.92	18.61

Table 4. Continued

Run No.	Q x 10^{-9}	q x 10^{-9}	q^2 x 10^{-18}	C_a	Vol x 10^{-3}	R	NOD	K_I x 10^{-3}	E	U_o
72	10.06	2.57	6.64	3.841	12.19	1.427	410	5.56	10.17	18.61
73	9.02	2.33	5.46	6.427	12.39	1.435	403	4.55	17.02	18.61
74	11.83	2.89	8.35	4.634	11.34	1.393	440	7.17	12.27	18.61
				F_a = 1690						
75	14.92	2.72	7.43	4.390	7.34	1.205	680	5.27	11.63	26.03
76	14.83	2.88	8.31	4.785	8.05	1.243	620	5.71	12.67	26.03
77	4.36	1.26	1.59	5.363	14.69	1.519	340	1.76	14.20	13.24
78	4.15	1.10	1.21	3.151	12.86	1.453	388	0.86	8.34	21.46
79	8.92	1.90	3.63	3.917	9.29	1.304	538	2.22	10.37	27.85
80	11.88	2.68	7.23	4.163	10.19	1.344	493	5.24	11.03	22.83
				- Volts						
81	11.97	2.88	8.31	2.559	11.11	1.384	450	5.32	6.77	25.11
82	7.01	1.86	3.47	1.165	12.86	1.453	388	2.06	3.08	25.80
83	13.83	2.95	8.73	2.826	9.28	1.303	538	5.78	7.48	25.80

Table 4. Continued

Run No.	Q x 10^{-9}	q x 10^{-9}	q^2 x 10^{-18}	C_a	Vol x 10^{-3}	R	NOD	K_I x 10^{-3}	E	U_o
84	10.13	2.61	6.82	1.749	12.30	1.431	406	4.11	4.63	25.80
85	3.23	0.88	0.77	0.407	13.41	1.473	372	0.45	1.07	25.80
86	9.17	2.29	5.24	1.571	11.73	1.409	426	3.20	4.16	25.80
87	0.43	0.11	0.01	0.094	12.90	1.454	387	0.00	0.24	23.97
88	9.47	2.28	5.23	2.278	11.16	1.386	447	3.50	6.03	23.97
89	12.36	2.73	7.47	3.847	9.77	1.326	511	5.23	10.19	23.97
90	2.95	0.78	0.61	0.858	12.80	1.451	390	0.39	2.27	23.97
91	10.43	2.52	6.37	4.025	11.18	1.387	447	4.26	10.66	23.97
92	4.81	1.26	1.60	2.070	12.67	1.446	394	1.02	5.48	23.97
93	11.61	2.73	7.45	5.553	10.71	1.367	466	5.06	14.71	23.97
94	3.41	0.90	0.81	1.775	12.70	1.450	390	0.53	4.70	23.29
95	8.60	2.15	4.63	7.211	11.78	1.411	424	3.13	19.10	23.29
				+ Volts						
96	1.32	0.39	0.15	2.050	15.46	1.545	323	0.13	5.43	16.44

Table 4. Continued

Run No.	Q x 10^{-9}	q x 10^{-9}	q^2 x 10^{-18}	C_a	Vol x 10^{-3}	R	NOD	K_I x 10^{-3}	E	U_o
97	11.13	2.90	8.44	6.313	12.53	1.440	378	7.93	16.72	16.44
98	5.41	1.57	2.47	4.421	14.70	1.519	339	2.20	11.71	16.44
99	14.59	3.37	11.38	11.36	10.44	1.355	478	11.70	30.07	15.98
100	6.94	1.92	3.69	6.491	13.68	1.483	365	3.36	17.19	16.44
101	11.06	2.71	7.35	20.62	11.40	1.396	438	6.75	54.61	17.35
102	6.12	1.71	2.94	4.334	13.95	1.493	358	2.66	11.48	16.44
103	13.38	3.20	1.02	8.934	11.00	1.379	454	10.66	23.66	15.53
104	10.09	2.58	6.68	9.090	12.19	1.427	410	6.91	24.07	15.07
				F_a = 1350						
105	18.17	2.89	8.36	7.294	5.96	1.124	837	6.36	19.32	26.03
106	12.41	2.82	7.97	6.453	10.20	1.345	489	5.34	17.09	24.66
107	6.79	1.75	3.07	3.702	12.31	1.432	406	2.01	9.80	23.74
108	14.38	2.93	8.60	8.250	8.65	1.273	577	6.52	21.85	23.06
109	5.45	1.43	2.05	3.749	12.69	1.446	393	1.39	9.92	22.60

Table 4. Continued

Run No.	Q x 10^{-9}	q x 10^{-9}	q^2 x 10^{-18}	C_a	Vol x 10^{-3}	R	NOD	K_I x 10^{-3}	E	U_o
110	14.54	3.09	9.58	9.925	9.23	1.301	541	7.25	26.28	22.60
111	14.80	3.16	10.04	4.981	9.31	1.305	536	7.65	15.84	22.37
112	18.05	4.70	22.17	2.364	12.52	1.440	399	15.16	6.26	22.60
113	2.95	0.54	0.30	7.099	7.54	1.216	663	0.24	18.80	22.60
114	23.35	5.97	35.74	4.446	12.17	1.426	410	24.69	11.77	22.60
115	6.02	1.28	1.66	7.350	9.31	1.305	536	1.26	19.47	22.37
116	18.97	5.12	26.30	2.099	13.21	1.466	378	17.85	5.56	22.37
117	1.26	0.27	0.07	3.069	9.78	1.326	511	0.35	8.12	37.21
118	6.18	0.77	0.59	3.418	4.16	0.997	1201	0.36	9.05	35.62
119	23.64	4.39	19.33	4.289	7.54	1.216	663	9.93	11.36	35.62
120	22.92	5.52	30.52	2.566	3.60	0.950	1385	65.26	6.79	10.96
121	9.25	1.85	3.45	2.605	8.46	1.264	590	2.21	6.89	27.40
				F_a = 1550						
122	11.80	3.12	9.75	4.065	12.79	1.450	390	7.45	10.77	20.09

Table 4. Continued

Run No.	Q x 10^{-9}	q x 10^{-9}	q^2 x 10^{-18}	C_a	Vol x 10^{-3}	R	NOD	K_I x 10^{-3}	E	U_o
123	11.99	2.53	6.40	5.946	9.11	1.295	548	4.58	15.75	23.97
124	13.45	2.69	7.23	5.250	8.40	1.261	594	4.54	13.90	28.08
125	11.60	2.96	8.80	5.933	12.15	1.426	411	4.45	15.71	30.82
126	0	0	0	0.245	12.81	1.451	390	0.00	0.65	26.03
127	17.99	4.80	23.10	2.392	12.97	1.457	385	13.56	6.33	26.03
128	17.99	4.55	20.70	2.474	11.95	1.418	418	13.56	6.55	23.97
129	13.72	2.65	7.06	3.601	8.01	1.241	623	5.96	9.53	21.00
130	9.66	2.29	5.24	2.828	10.84	1.372	461	4.04	7.49	21.00
131	12.83	2.76	7.64	3.251	9.40	1.309	531	6.18	8.60	21.00
132	7.50	1.88	3.53	3.228	12.02	1.421	423	2.47	8.54	22.37
133	0	0	0	0.252	13.72	1.485	364	0.00	0.66	31.96
134	9.60	1.77	3.15	3.012	7.47	1.212	668	1.90	7.97	30.37
135	14.62	3.13	9.84	4.747	9.32	1.305	536	8.34	12.57	20.09
136	14.63	3.13	9.84	4.892	9.32	1.305	535	8.35	12.96	20.09

Table 4. Continued

Run No.	Q x 10^{-9}	q x 10^{-9}	q^2 x 10^{-18}	C_a	Vol x 10^{-3}	R	NOD	K_I x 10^{-3}	E	U_o
137	0	0	0	0.858	12.82	1.451	389	0.00	2.27	26.03
138	9.62	2.58	6.68	3.318	13.07	1.461	382	4.24	8.78	23.97
139	13.83	1.82	3.34	3.472	9.00	1.290	555	2.74	9.19	21.00
140	13.27	2.46	6.09	4.042	7.54	1.216	662	5.3	10.70	21.00

BIBLIOGRAPHY

1. Fuchs, N. A., The Mechanics of Aerosols, Pergamon Press, Inc., New York, New York (1964).

2. Davies, C. N., (edited), Aerosol Science, Academic Press, New York, New York (1966).

3. Green, H. L. and Lane, W. R., Particulate Clouds: Dusts, Smokes, and Mists, 2nd ed., D. Van Nostrand Company, Inc., Princeton, New Jersey (1964).

4. Wilson, I. B., quoted in (2), pp 78.

5. Davies, C. N., quoted in (1), pp 173.

6. Fuchs, N. A. and others, "On the Determination of Particle Size Distribution in Polydisperse Aerosols by the Diffusion Method," Brit. J. Appl. Phys., 1962, 13, 280.

7. Zebel, G., "Deposition of Aerosol Flowing Past a Cylindral Fiber in a Uniform Electric Field," J. Coll. Sci., 1965, 20, 522.

8. Natanson, G. L., quoted in (2), pp 75.

9. Walton, W. H. and Woolcock, A., "The Suppression of Airborne Dust by Water Spray," Int. J. Air Poll., 1960, 3, 129.

10. Picknett, R. G., "Collection Efficiences For Water Drops in Air," Int. J. Air Poll., 1960, 3, 160.

11. Khimach, M. and Shishkin, N., quoted in (1), pp 167.

12. Pemberton, C. S., "Scavenging Action of Rain on Non-Wettable Particulate Matter Suspended in the Atmosphere," Int. J. Air Poll., 1960, 3, 165.

13. Oakes, B., "Laboratory Experiments Relating to the Wash-Out of Particles by Rain," Int. J. Air Poll., 1960, 3, 179.

14. Herne, H. and Fonda, G., "The Classical Computations of the Aerodynamic Capture of Particles by Spheres," Int. J. Air Poll., 1960, 3, 26.

15. Lundgren, D. A. and Whitby, K. T., quoted in (2), pp 75.

16. Gillespie, T., "Electric Charge Effects in Aerosol Collision Phenomena," Int. J. Air Poll., 1960, 3, 44.

17. Gunn, K. and Hitschfeld, W., "A Laboratory Investigation of the Coalescence Between Large and Small Water Drops," J. Meteor., 1951, 8, 7.

18. Kraemer, H. and Johnstone, H., "Collection of Aerosol Particles in Presence of Electric Fields," Ind. Eng. Chem., 1955, 47, 2426.

19. Licht, W. and Conway, J. B., "Mechanism of Solute Transfer in Spray Towers," Ind. Eng. Chem., 1950, 42, 1151.

20. Licht, W. and Pansing, W. F., "Solute Transfer From Single Drops in Liquid-Liquid Extraction," Ind. Eng. Chem., 1953, 45, 1885.

21. Giardina, P. J., "The Effects of Humidity and Gas Phase Concentration on the Absorption of Sulfur Dioxide by Charged Aqueous Droplets," Master's Thesis in Chemical Engineering, Georgia Institute of Technology, 1973.

22. Beers, Y., Theory of Error, Addison-Wesley Publishing Company, Cambridge, Massachusetts (1953), pp 34.

23. Chow, H. Y. and Mercer, T. T., "Charges on Droplets Produced by Atomization of Solutions," Amer. Ind. Hygiene Ass. J., 1971, 32, 247.